Universitat de Girona

NUR MUHAMMAD

Impact of thermal degradation on the glass transition temperature and viscoelastic behavior of an epoxy-based vitrimer resin



FRP++
Advanced structural analysis and design using composite materials

Master Dissertation
European Master Advanced Structural Analysis and Design using Composite Materials

Work developed under the supervision of
Professor Doctor Laura Carreras
Professor Doctor Daniel Sánchez Rodríguez



Funded by the European Union

September 2026

DECLARATION

Name: NUR MUHAMMAD

Email: nuryzu7@gmail.com **Phone number: +34 7 11 21 86 50**

Title of the Dissertation: Impact of thermal degradation on the glass transition temperature and viscoelastic behavior of an epoxy-based vitrimer resin

Supervisors:

Professor Doctor Laura Carreras

Professor Doctor Daniel Sánchez Rodríguez

Year of Conclusion: 2026

Master Course in Advanced Structural Analysis and Design using Composite Materials

THE ENTIRE REPRODUCTION OF THIS DISSERTATION IS AUTHORIZED ONLY FOR RESEARCH PURPOSES, UPON WRITTEN DECLARATION BY THE INTERESTED PERSON, WHICH IS COMMITTED TO.

University of Girona, 27/08/2026

Signature: 

ACKNOWLEDGEMENTS

First, I would like to express my sincere gratitude to the FRP++ team, especially Professor José Sena Cruz, Professor Luís Correia, Professor Bruno Castanié, and Professor Cristina Barris, for giving me the opportunity to be part of this outstanding master's program. I am truly grateful for their trust, support, and for the academic environment they created throughout this journey.

I am especially thankful to my supervisors, Professor Laura Carreras and Professor Daniel Sánchez Rodríguez, for their guidance, patience, encouragement, and continuous support throughout the development of this dissertation. Their advice and dedication were invaluable in helping me complete this work, while their genuine kindness and unconditional support, both academically and personally, inspired me throughout the entire journey. A very special thanks goes to Sihem Zaidi, who has been not only a mentor but also a true friend. Her support, encouragement, and guidance throughout this journey meant a great deal to me, both academically and personally.

I would also like to thank all my professors, classmates, and friends who contributed in different ways to this experience. Their support, companionship, discussions, and encouragement made the entire program more meaningful and memorable.

My sincere appreciation also goes to everyone who assisted me with the academic and administrative procedures throughout the master's program. In particular, I would like to thank Karine for her constant help, availability, and support during the different stages of the program.

Finally, I would like to express my deepest gratitude to my family for their unconditional love, patience, and support throughout this journey. I am especially grateful to my mother, whose encouragement, strength, and constant belief in me have been a source of motivation during both the most rewarding and the most challenging moments. Her support has meant more to me than words can fully express, and I dedicate this achievement to her with all my heart.

Impacto de la degradación térmica en la temperatura de transición vítrea y el comportamiento viscoelástico de una resina vitrímera de base epoxi

RESUMEN

Los vitrímeros epoxi combinan la estabilidad mecánica de los termoestables con reacciones de intercambio de enlaces activadas térmicamente, que permiten la relajación de tensiones y el reprocesado. Sin embargo, las altas temperaturas necesarias para activar estos procesos también pueden favorecer una degradación térmica irreversible. Esta disertación estudia cómo dicha degradación afecta a la temperatura de transición vítrea, T_g, y al comportamiento viscoelástico de un vitrímero epoxi basado en disulfuros aromáticos. La cinética de degradación térmica se caracterizó mediante análisis termogravimétrico (TGA) y la relajación de tensiones mediante análisis mecánico dinámico (DMA). Ambos procesos se analizaron con el método isoconversional de Friedman y se combinaron en un diagrama tiempo–temperatura–transformación (TTT). El modelo reprodujo adecuadamente la relajación a temperaturas superiores a T_g, pero mostró desviaciones cerca de la transición vítrea, donde la movilidad segmentaria adquiere mayor influencia. Posteriormente, se realizaron tratamientos térmicos a 220 °C para generar distintos niveles de degradación. El módulo de almacenamiento disminuyó de aproximadamente 5430 a 3240 MPa tras 2 h de exposición, mientras que T_g se redujo alrededor de 30 °C para grados de degradación del 4–6 %. A mayores niveles de degradación, ambas propiedades mostraron un comportamiento no monótono. En conjunto, los resultados establecen una relación directa entre la degradación térmica y la pérdida de propiedades físicas, proporcionando una base para definir condiciones más seguras de procesado y reprocesado de vitrímeros epoxi.

PALABRAS CLAVE: Vitrímero epoxi; Degradación térmica; Relajación de tensiones; Análisis mecánico dinámico; Análisis isoconversional; Diagrama tiempo–temperatura–transformación (TTT)

Impacte de la degradació tèrmica en la temperatura de transició vítria i el comportament viscoelàstic d'una resina vitrímera de base epoxi

RESUM

Els vitrimers epoxi combinen l'estabilitat mecànica dels termoestables amb reaccions d'intercanvi d'enllaços activades tèrmicament, que permeten la relaxació de tensions i el reprocessament. Tanmateix, les temperatures necessàries per activar aquests processos també poden afavorir una degradació tèrmica irreversible. Aquesta dissertació analitza com aquesta degradació afecta la temperatura de transició vítria, T_g, i el comportament viscoelàstic d'un vitrimer epoxi basat en disulfurs aromàtics. La cinètica de degradació tèrmica es va caracteritzar mitjançant anàlisi termogravimètrica (TGA) i la relaxació de tensions mitjançant anàlisi mecànica dinàmica (DMA). Ambdós processos es van analitzar amb el mètode isoconversional de Friedman i es van combinar en un diagrama temps–temperatura–transformació (TTT). El model va descriure adequadament la relaxació a temperatures superiors a T_g, però va mostrar desviacions a prop de la transició vítria, on la mobilitat segmentària té una influència més gran. Posteriorment, es van realitzar tractaments tèrmics a 220 °C per generar diferents nivells de degradació. El mòdul d'emmagatzematge va disminuir d'aproximadament 5430 a 3240 MPa després de 2 h d'exposició, mentre que $T_g$es va reduir aproximadament 30 °C per a graus de degradació del 4–6 %. A nivells de degradació més elevats, ambdues propietats van mostrar un comportament no monòton. En conjunt, els resultats estableixen una relació directa entre la degradació tèrmica i la pèrdua de propietats físiques, proporcionant una base per definir condicions més segures de processament i reprocessament de vitrimers epoxi.

PARAULES CLAU: Vitrimer epoxi; Degradació tèrmica; Relaxació de tensions; Anàlisi mecànica dinàmica; Anàlisi isoconversional; Diagrama temps–temperatura–transformació(TTT)

Impact of thermal degradation on the glass transition temperature and viscoelastic behavior of an epoxy-based vitrimer resin

ABSTRACT

Epoxy vitrimers combine the mechanical stability of thermosets with thermally activated bond-exchange reactions that enable stress relaxation and reprocessing. However, the elevated temperatures required for these processes can also promote irreversible thermal degradation. This dissertation investigates how thermal degradation affects the glass transition temperature and viscoelastic behavior of an aromatic disulfide-based epoxy vitrimer. Thermal-degradation kinetics were characterized by thermogravimetric analysis (TGA), while stress-relaxation kinetics were determined by dynamic mechanical analysis (DMA). Both processes were analyzed using Friedman's isoconversional method and combined in a time–temperature–transformation (TTT) diagram to define the competition between network relaxation and degradation. The isoconversional description reproduced stress-relaxation behavior well at temperatures sufficiently above T_g, but became less reliable near the glass-transition region, where segmental mobility increasingly influences the relaxation response. Controlled thermal treatments at 220 °C were then used to generate different degradation states. The storage modulus decreased from approximately 5430 MPa for the undegraded material to 3240 MPa after 2 h of exposure, while T_g decreased by about 30 °C at approximately 4–6% degradation. At higher degradation levels, both properties showed non-monotonic behavior, indicating a more complex evolution of the polymer network. The study establishes a direct link between degradation kinetics and physical property loss, providing a more robust basis for defining safe processing and reprocessing conditions for epoxy vitrimers.

KEYWORDS: Epoxy vitrimer; Thermal degradation; Stress relaxation; Dynamic mechanical analysis; Isoconversional analysis; Time–temperature–transformation (TTT) diagram;

TABLE OF CONTENTS

Acknowledgements III
Resumen IV
Resum V
Abstract VI
List of Figures IX
List of Abbreviations and Symbols XI
1. Introduction 1
1.1. Motivation and Objectives 1
1.2. Literature Review 2
1.2.1. Thermosetting Polymers and the Recyclability Challenge 2
1.2.2. Covalent Adaptable Networks (CANs) as a Sustainable Alternative 3
1.2.3. Vitrimers: Concept and Exchange Chemistries 5
1.2.4. Epoxy-Based Vitrimers 10
1.2.5. Processing and Reprocessing of Vitrimers: The Role of Thermal Degradation 11
1.2.6. Self-healing and reshaping properties 12
1.2.7. Effects of Thermal Degradation on Physical and Mechanical Properties 14
1.2.8. Research Gap 15
2. Materials and methods 17
2.1. Materials 17
2.2. Formulation and Curing Process 17
2.3. Isoconversional Kinetic Analysis 18
2.3.1. Defining the extent of transformation from DMA and TGA data 18
2.3.2. The isoconversional hypothesis 20
2.3.3. The rate equation and Friedman's linearization 20
2.3.4. Predicting isothermal behavior from the extracted kinetic parameters 21
2.3.5. Extending the prediction to arbitrary (non-isothermal) temperature profiles 21
2.4. Methods 22
2.4.1. Thermogravimetric Analysis (TGA) 22
2.4.2. Controlled Thermal Degradation (Oven Treatment) 22

2.4.3. Dynamic Mechanical Analysis (DMA) 23
3. Results and discussion 24
3.1. Thermal Degradation Behavior (TGA) 24
3.1.1. Normalized TGA Curves at Multiple Heating Rates 24
3.2. Isoconversional Kinetic Analysis of Degradation 26
3.2.1. Friedman Analysis: Apparent Activation Energy vs. Degree of Degradation 26
3.3. Dynamic Mechanical Analysis of Pristine and Degraded Specimens 29
3.3.1. DMA Friedman/Isoconversional Analysis 29
3.4. Time–Temperature–Transformation (TTT) Map 34
3.4.1. Construction of the TTT Diagram 34
3.4.2. Selection of Oven-Treatment Conditions from the TTT Map 36
3.5. Evolution of Storage Modulus with Degradation 38
3.5.1. E′ vs. Degradation Time from DMA Double-Cantilever Measurements 38
3.5.2. Discussion: Stiffness Loss Mechanisms 40
3.6. Evolution of Glass Transition Temperature with Degradation 42
3.6.1. Tg vs. Degree of Thermal Degradation 42
3.6.2. Discussion: Correlating Tg Loss with Network Degradation Kinetics 44
3.7. Linking Degradation Kinetics to Physical Property Loss 47
4. Conclusion 52
4.1. Summary of Findings 52
4.2. Future Work 53

LIST OF FIGURES

Figure 1-1 Classification of dynamic covalent bonds (DCBs) according to reaction type, covalent adaptable network mechanism, complementarity of reactive units, and their functional objective [12] 4
Figure 1-2 Schematic illustration of dissociative and associative exchange mechanisms in vitrimeric polymer networks 4
Figure 1-3 Schematic illustration of the reprocessing and recycling pathways of vitrimeric materials [19] 6
Figure 1-4 Classification of vitrimer bond-exchange reactions according to catalytic requirements, distinguishing catalyst-assisted and catalyst-free pathways [25] 7
Figure 1-5 Overview of elastic modulus versus healing temperature of a wide range of intrinsic self-healing polymer matrices developed in the past decade [26] 7
Figure 2-1 Curing and sample preparation process of the epoxy-based vitrimer resin, including formulation, curing, demolding, and preparation of specimens for characterization 17
Figure 2-2 Schematic representation of the thermogravimetric analysis (TGA) principle used to characterize the thermal degradation behavior of the cured vitrimer resin 20
Figure 3-1 Normalized mass-loss curves of the cured epoxy vitrimer obtained by TGA at different heating rates (1.25, 2.5, 5, 10, and 20 °C/min) 26
Figure 3-2 Apparent activation energy, (E_α), as a function of the degree of thermal degradation obtained using Friedman's isoconversional analysis 28
Figure 3-3 Comparison between experimentally measured and isoconversionally predicted stress-relaxation behavior of the pristine epoxy vitrimer at temperatures above the glass transition region 29
3-4 Apparent activation energy, ($E\alpha$), of the stress-relaxation process and corresponding Friedman correlation coefficient as a function of the degree of conversion 31
Figure 3-5 Comparison between experimentally measured and isoconversionally predicted stress-relaxation behavior of the pristine epoxy vitrimer at temperatures close to the glass transition region 32
Figure 3-6 Time–temperature–transformation (TTT) diagram showing the predicted stress-relaxation and thermal-degradation kinetics of the epoxy vitrimer 36

Figure 3-7 Visual appearance of the pristine and thermally treated epoxy vitrimer specimens after exposure at 220 °C for 30 min, 1 h, 2 h, and 4 h. The undegraded specimen is shown on the left 38
Figure 3-8 Evolution of the storage modulus, (E'), with degradation time for pristine and thermally degraded epoxy vitrimer specimens treated at 220 °C 40
Figure 3-9 Glass transition temperature, (Tg), as a function of the degree of thermal degradation for pristine and thermally degraded epoxy vitrimer specimens 44

LIST OF ABBREVIATIONS AND SYMBOLS

Abbreviation	Definition
APhD	4-Aminophenyl disulfide
BGPDS	Bis(4-glycidyloxyphenyl)disulfide
DCB	Dynamic covalent bonding
CAN	Covalent Adaptable Network
CFRP	Carbon Fibre-Reinforced Polymer
DBU	Diazabicycloundecene
DGEBA	Diglycidyl Ether of Bisphenol A
DMA	Dynamic Mechanical Analysis
DPDS	Diphenyl disulfide
FTIR	Fourier-Transform Infrared Spectroscopy
ILSS	Interlaminar Shear Strength
PCL	Polycaprolactone
PEI	Polyethylenimine
TA	Thermal Analysis
TBP	Tributylphosphine
DSC	Differential Scanning Calorimetry
TGA	Thermogravimetric Analysis
TTT	Time–Temperature–Transformation
UV	Ultraviolet

Symbol	Definition	Typical unit
A_α	Pre-exponential factor at a given degree of conversion	Depends on kinetic formulation
E_α	Apparent activation energy at conversion α	kJ·mol^{-1}
E'	Storage modulus	MPa
E''	Loss modulus	MPa

Symbol	Definition	Typical unit
$f(\alpha)$	Reaction-model function at conversion α	–
m_i	Initial sample mass	mg or g
m_f	Final sample mass	mg or g
R	Universal gas constant	J·mol^{-1}·K^{-1}
t	Time	s, min, or h
T	Absolute temperature	K
T_g	Glass transition temperature	°C
T_v	Topology freezing transition temperature	°C
α	Degree of transformation/conversion; represents stress-relaxation conversion or degree of thermal degradation depending on context	–
β	Heating rate, dT/dt	°C·min^{-1} or K·min^{-1}
δ	Phase angle between applied deformation and material response in DMA	° or rad
$\Delta\alpha$	Increment in degree of conversion	–
Δt	Time increment	s
$d\alpha/dt$	Transformation or conversion rate	s^{-1}
σ	Stress / stress-relaxation response	Pa or MPa
$\tan\delta$	Loss factor	–

1. INTRODUCTION

1.1. Motivation and Objectives

Thermosetting polymers are widely used in structural applications due to their outstanding mechanical properties, thermal stability, and chemical resistance. However, their permanently cross-linked network structure prevents reforming, reprocessing, or recycling once cured, making them a growing source of non-degradable waste as their industrial use continues to expand.

Vitrimers address this limitation by incorporating dynamic covalent bonds into the cross-linked network, allowing the material to undergo reversible topological rearrangement when heated above a characteristic transition temperature. This exchange behavior grants vitrimers the ability to be reshaped, self-healed, and reprocessed multiple times while retaining the mechanical performance typical of conventional thermosets, positioning them as a promising, more sustainable alternative for structural composite applications.

However, both the initial curing of epoxy-based vitrimers and their subsequent reprocessing require elevated temperatures to activate the exchange reactions. At these temperatures, the network's dynamic rearrangement competes directly with thermal degradation of the polymer. Vitrimers based on functional epoxy groups DGEBA (Araldite LY1564) and 4-Aminophenyl disulfide designed for structural applications typically require relatively high glass transition temperatures, which in turn necessitate reprocessing at elevated temperatures where thermal degradation becomes a significant concern. Thus, making the assessment of the material's degradation kinetics and thermal stability particularly relevant.

Prior work has investigated the thermal degradation kinetics of epoxy vitrimers and has developed processing and reprocessing maps to help identify safe time-temperature windows for curing and reshaping [1]. Separately, other studies have examined how elevated processing temperatures affect the mechanical properties and thermal stability of epoxy resins in general [2-4]. However, a direct, quantitative link between the degree of thermal degradation experienced by a vitrimer and the resulting evolution of its glass transition temperature and viscoelastic properties has not yet been fully characterized.

This dissertation aims to establish this link for an aromatic disulfide-containing epoxy vitrimer by correlating controlled, quantified degrees of thermal degradation with the resulting changes in glass transition temperature and viscoelastic behavior. To achieve this, the thermal degradation kinetics of the studied vitrimer are first characterized using thermogravimetric analysis (TGA) and Friedman's isoconversional method, while the kinetics of stress relaxation are independently characterized through dynamic mechanical analysis (DMA) using the same isoconversional approach. The kinetic parameters obtained from both analyses are then combined to construct a time–temperature–transformation (TTT) map that simultaneously describes the stress-relaxation and thermal-degradation kinetics, thereby providing a basis for identifying suitable processing and reprocessing conditions. Specimens with controlled and quantified degrees of thermal degradation are subsequently generated through isothermal oven treatments selected using the degradation kinetics. The evolution of the glass transition temperature and viscoelastic properties of the degraded specimens is then determined through DSC and DMA in a dual-cantilever configuration respectively. Finally, a quantitative correlation is established between the degree of thermal degradation, the glass transition temperature, and the viscoelastic properties of the vitrimer, providing a more complete basis for assessing the consequences of thermal exposure and supporting the design of safer processing and reprocessing conditions for this class of materials.

1.2. Literature Review

1.2.1. Thermosetting Polymers and the Recyclability Challenge

Several strategies have historically been employed to manage thermoset waste, including mechanical grinding for use as filler material, pyrolysis, and solvolysis-based chemical recycling. Mechanical recycling typically yields only low-value filler products, as the resulting particles lack the load-bearing capacity of the original material. Pyrolysis and solvolysis can recover some raw materials or reinforcing fibers, but these processes are energy-intensive, often require harsh chemical conditions, and generally fail to preserve the resin itself for reuse [5, 6]. As a result, the overwhelming majority of thermoset composite waste continues to be disposed of through landfill or incineration, despite growing volumes generated by industries

such as aerospace, automotive, and wind energy, where thermoset composites are used extensively for their strength-to-weight advantages.

This waste burden has become increasingly difficult to reconcile with tightening environmental regulations and end-of-life directives across major manufacturing sectors, which are pushing industry toward circular economy principles and away from landfill-dependent material lifecycles. At the same time, replacing thermosets outright with thermoplastics is not a viable general solution, since thermoplastics typically cannot match the crosslink-derived mechanical strength, creep resistance, and thermal stability that structural applications require.

This combination of factors, a mature and irreplaceable material class with a fundamentally unsolved end-of-life problem, has driven sustained research interest in an entirely different approach: redesigning the crosslinked network itself so that it can be broken down and reformed on demand, without sacrificing the mechanical performance thermosets are valued for [7]. This is the motivation behind covalent adaptable networks, discussed in the following section.

1.2.2. Covalent Adaptable Networks (CANs) as a Sustainable Alternative

Covalent adaptable networks (CANs) were introduced as a class of polymer networks in which the cross-linking points of an otherwise permanently cured material are able to undergo reversible rearrangement reactions, thereby granting the network macroscopic flow and stress relaxation capability despite remaining covalently bonded at all times. This concept fundamentally redefines what a cross-linked network can do: rather than being locked into a single, permanent topology upon curing, a CAN can be selectively activated, typically by heat, light, or another external stimulus, to reorganize its internal connectivity while preserving its overall crosslink density and structural integrity [8-11].

CANs are broadly classified according to the mechanism by which their bond exchange proceeds (Figure 1-2) [12]. In dissociative networks, an existing bond must first be broken before a new one forms, resulting in a transient decrease in crosslink density during the exchange process. In associative networks, by contrast, a new bond forms before or simultaneously with the breaking of the old one, so that the network's crosslink density, and therefore its mechanical integrity, remains essentially constant throughout the

rearrangement process. This associative behavior is particularly desirable for reprocessing applications, as it allows the material to flow and be reshaped without passing through a mechanically weakened intermediate state [13].

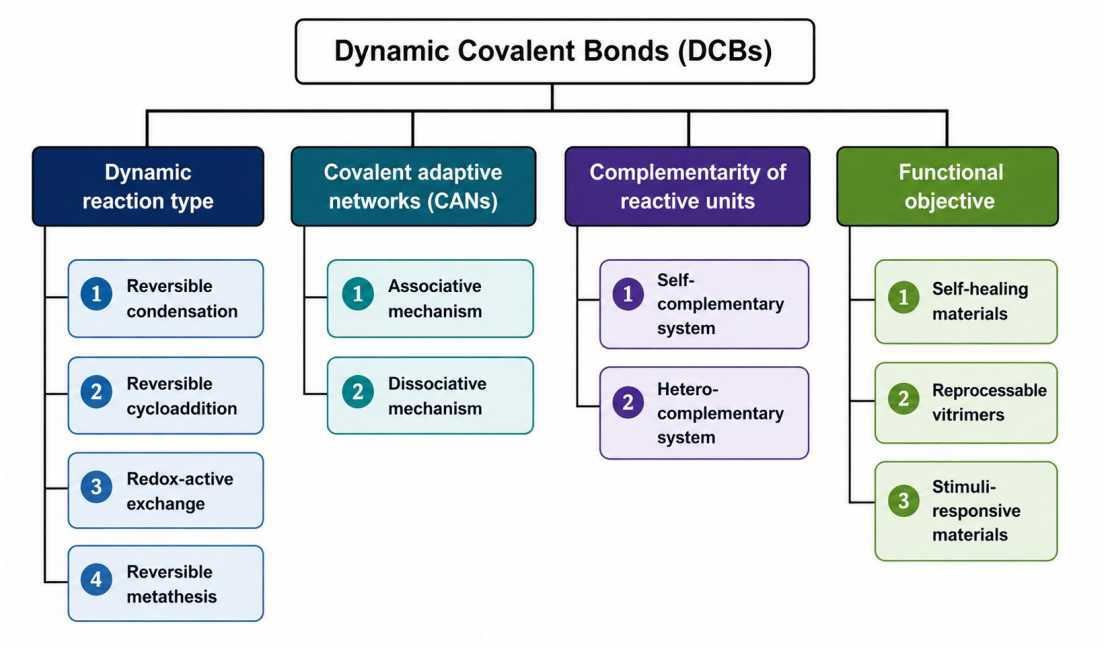


Figure 1-1 Classification of dynamic covalent bonds (DCBs) according to reaction type, covalent adaptable network mechanism, complementarity of reactive units, and their functional objective [12]

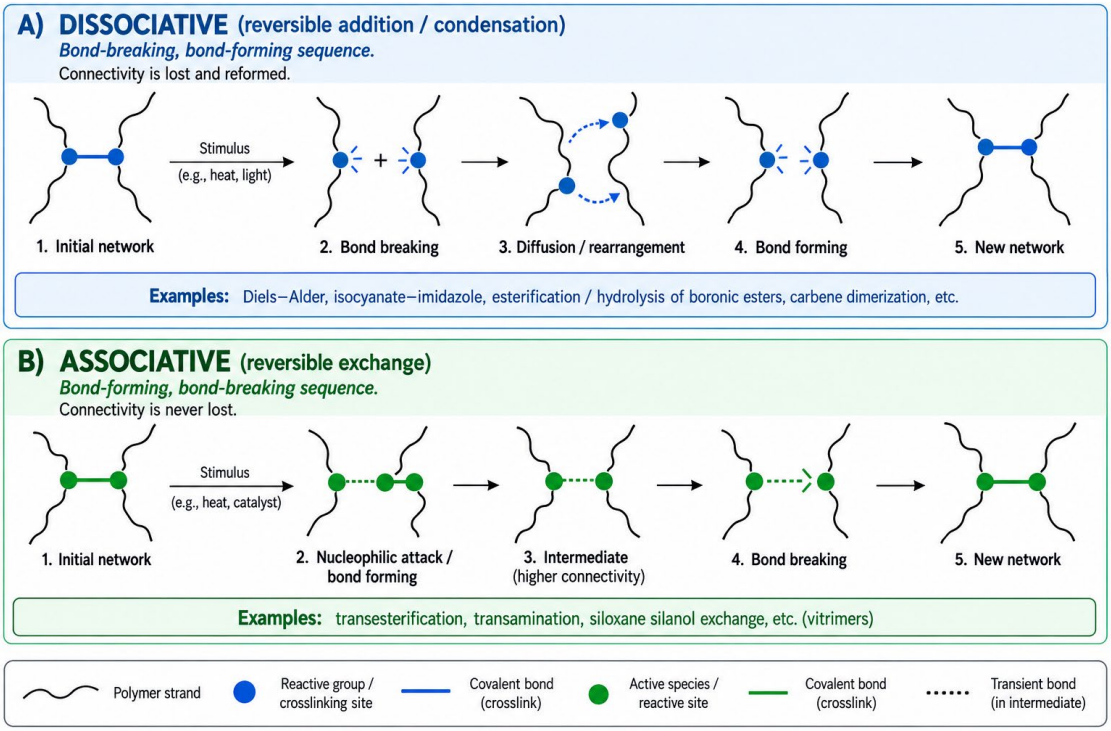


Figure 1-2 Schematic illustration of dissociative and associative exchange mechanisms in vitrimeric polymer networks

A wide range of reversible exchange chemistries has been reported for the preparation of CANs, including transesterification, transamination, disulfide exchange, siloxane equilibrium, amine-urea exchange, and transcarbamoylation [14-16]. Some of these exchange reactions require the presence of a catalyst, such as hydroxy ester or thiourethane-based systems, while others, notably imine and disulfide exchange, proceed without any catalyst under moderate heating. This catalyst-free reactivity is an important practical advantage, as it simplifies formulation, avoids potential catalyst leaching or toxicity concerns, and broadens the range of curing agents that can be used to prepare the network [17].

Among the many polymer platforms explored as CANs, epoxy-based systems have emerged as particularly attractive candidates, given the maturity of epoxy chemistry, the wide availability of epoxy monomers and curing agents, and the direct compatibility of CAN chemistry with existing epoxy processing infrastructure. Vitrimer refers to a polymer network with dynamic covalent bonds (Figure 1-1) that can exchange while maintaining network connectivity, discussed in detail in the following section.

1.2.3. Vitrimers: Concept and Exchange Chemistries

General Definition and Properties

Vitrimers were first introduced by Ludwik Leibler and coworkers as a distinct subclass of covalent adaptable networks, characterized by an associative exchange mechanism in which crosslink density remains constant throughout the rearrangement process [15, 16, 18]. Unlike conventional thermosets, which behave as rigid, permanently fixed networks at all service temperatures, vitrimers exhibit a gradual, Arrhenius-type increase in chain mobility as temperature rises, closely resembling the viscosity behavior of inorganic glasses such as silica. This behavior is captured by the concept of a topology freezing transition temperature (Tv), defined as the temperature at which the material's viscosity reaches approximately 10^{12} Pa·s [18]. Below Tv, the exchange reactions proceed too slowly to allow appreciable macroscopic flow, and the material behaves as a conventional cross-linked solid. Above Tv, bond exchange becomes kinetically significant, and the network can gradually flow, relax internal stresses, and be reshaped, while its overall crosslink density and covalent connectivity remain essentially unchanged [19-24]. This combination of thermoset-like mechanical performance

below Tv and thermoplastic-like reprocessability above it is what makes vitrimers particularly attractive as a sustainable alternative to conventional thermosetting resins.

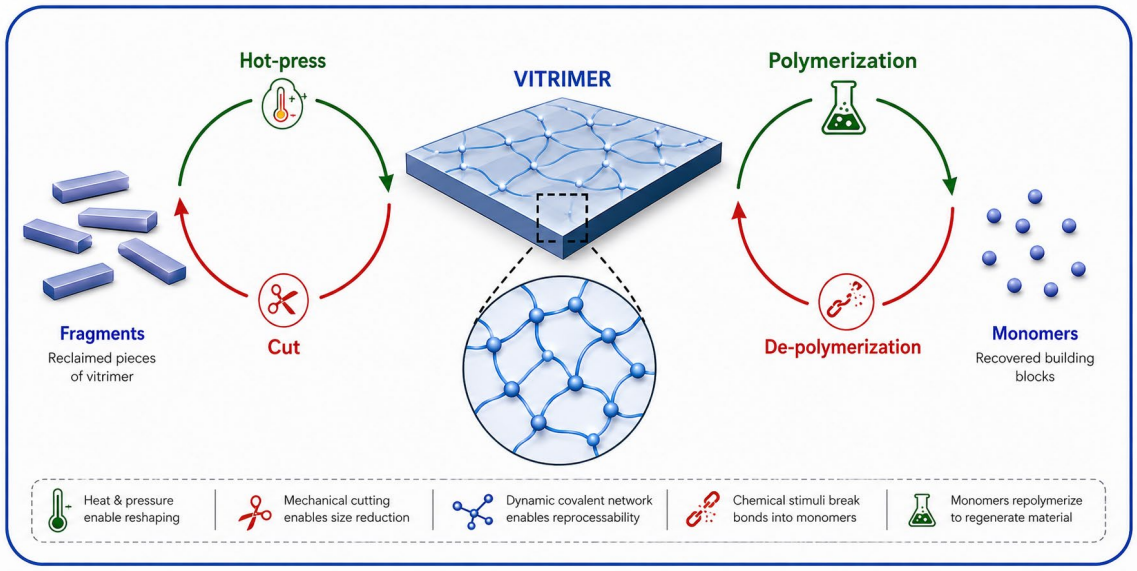


Figure 1-3 Schematic illustration of the reprocessing and recycling pathways of vitrimeric materials [19]

Variety of Dynamic Polymer Chemistry

The vitrimer concept has since been extended to a wide range of exchangeable chemistries beyond the original transesterification-based systems. Reported exchange mechanisms include transamination, siloxane equilibrium, amine-urea exchange, transcarbamoylation, and boronic ester exchange, each offering a different balance of exchange rate, activation energy, and processing temperature window. Some of these mechanisms require the presence of a catalyst to proceed at practical rates, such as the hydroxy ester and thiourethane-based systems commonly used in transesterification vitrimers, while others, notably imine and disulfide exchange, are able to proceed without any added catalyst under moderate heating. This diversity of exchange chemistries allows the vitrimer concept to be tailored to a broad range of polymer backbones and target applications, and has motivated substantial research interest in identifying which chemistries offer the best combination of fast relaxation, high thermal stability, and straightforward synthesis. Among these, disulfide and imine exchange have received particular attention within the epoxy vitrimer literature, owing to their catalyst-free operation and their compatibility with standard epoxy curing procedures.

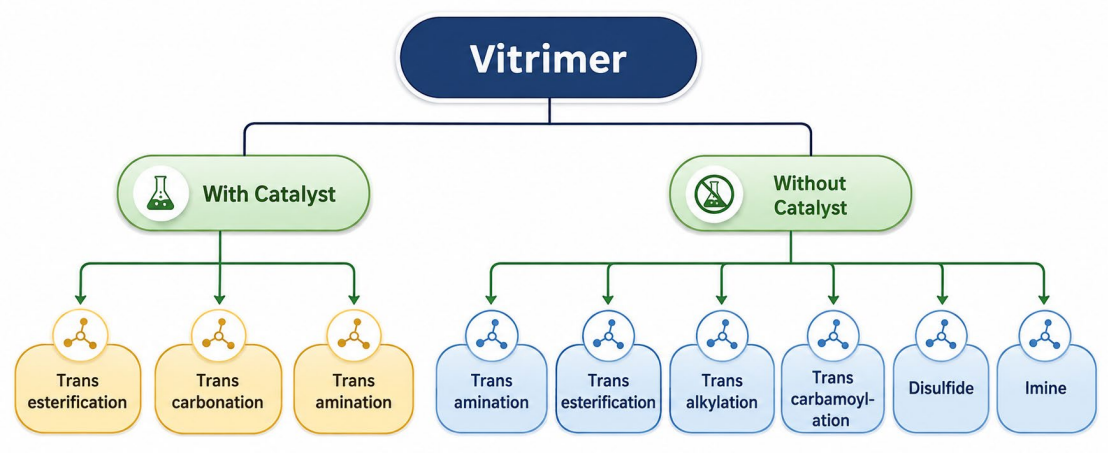


Figure 1-4 Classification of vitrimer bond-exchange reactions according to catalytic requirements, distinguishing catalyst-assisted and catalyst-free pathways [25]

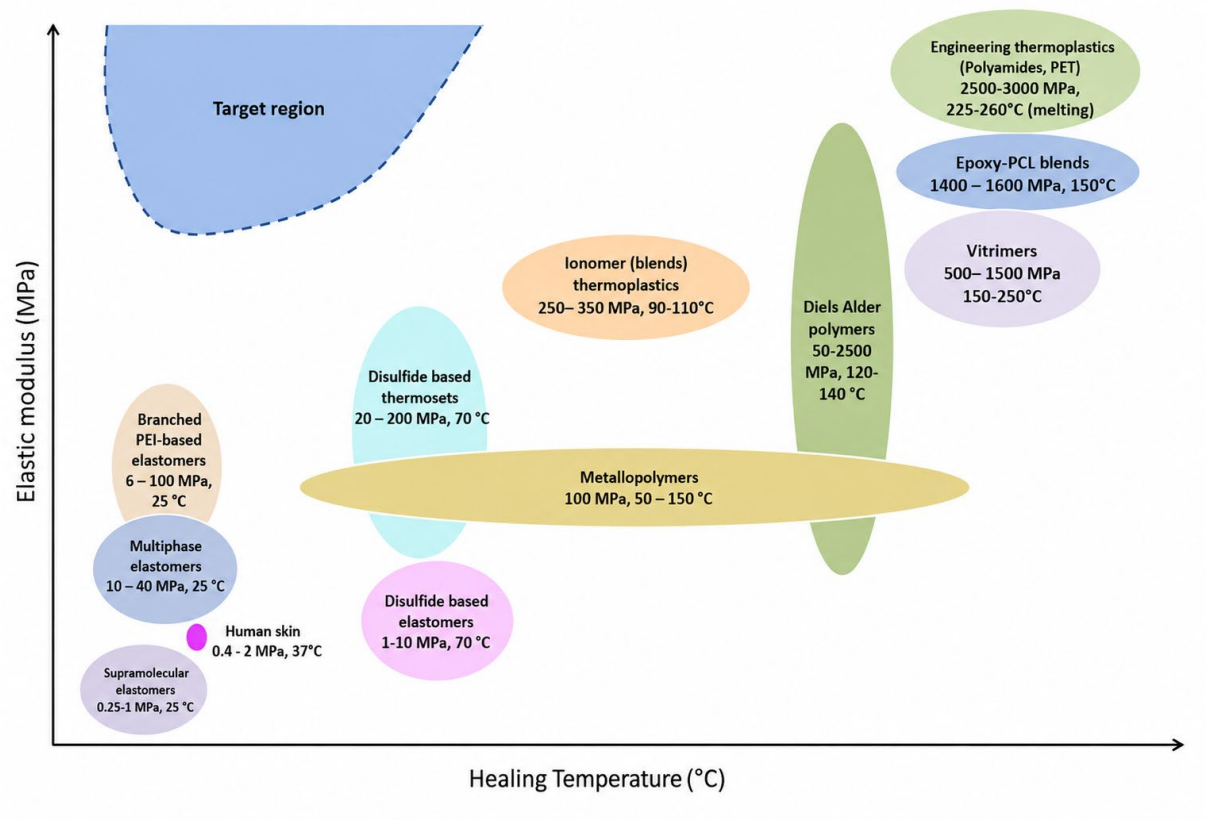


Figure 1-5 Overview of elastic modulus versus healing temperature of a wide range of intrinsic self-healing polymer matrices developed in the past decade [26]

In intrinsic self-healing polymers, there's a persistent trade-off: materials with a high room-temperature elastic modulus tend to need a high healing temperature, and vice versa. A comparison across major systems studied to date such as branched PEI elastomers, multiphase and supramolecular elastomers, human skin, disulfide-based elastomers, metallopolymers, ionomers and ionomer blends, Diels-Alder polymers, epoxy-PCL blends,

vitrimers, and disulfide-based epoxy thermosets, alongside engineering thermoplastics at their melting points for reference, shows that no system yet combines high modulus with low healing temperature the way commercial high-performance polymers do. That combination remains the central challenge in the field. Disulfide-based epoxy thermosets currently come closest to this target region, making them a promising starting point for developing self-healing fibre composites with strong mechanical properties.

Disulfide Exchange Mechanism

Disulfide bonds undergo a metathesis reaction in which one disulfide linkage exchanges with another, either through a radical-mediated pathway or through a nucleophilic substitution mechanism depending on the specific molecular environment. Aromatic disulfides, such as those derived from 4-aminophenyl disulfide, have proven especially effective for vitrimer applications, as the electron-withdrawing character of the aromatic ring stabilizes the radical or thiolate intermediate formed during exchange, allowing the reaction to proceed rapidly without a catalyst [27-29]. Epoxy vitrimers incorporating aromatic disulfide hardeners have been reported to achieve stress relaxation times as short as a few tens of seconds even without catalytic assistance, with apparent activation energies for the exchange reaction typically falling in the range of 45 to 190 kJ/mol, depending on the specific disulfide structure and surrounding network [17]. This combination of fast, catalyst-free relaxation and compatibility with conventional epoxy processing has made aromatic disulfide exchange one of the most widely studied and industrially relevant mechanisms for epoxy vitrimer development, including the CIDETEC-patented formulation examined in the present work.

Disulfide exchange chemistry is a well-established dynamic covalent approach that has attracted considerable attention due to its straightforward implementation and the relatively easy availability of its precursors [17, 29-32]. Moreover, disulfide chemistry has been extensively investigated because of its widespread application in the production of vulcanized rubber. Recent studies have demonstrated that covalent disulfide exchange is a complex process that can proceed through multiple mechanisms. Among these, a [2+1] radical-mediated pathway is considered one of the most probable mechanisms, with its occurrence being strongly influenced by the reaction conditions and the substitution patterns of the disulfide groups [27]. Despite its advantages and widespread use, this chemistry presents several limitations. In particular, free thiol groups are readily oxidized in the presence of

atmospheric oxygen, which can result in a significant deterioration of the dynamic properties over time. Additionally, the thermal stability of the S–S bond must be carefully considered, as disulfide bonds are susceptible to temperature-induced degradation, potentially leading to a gradual loss of the material's dynamic properties [33].

The dynamic exchange of disulfide bonds has been extensively investigated and documented in the literature. This type of exchange represents an associative mechanism characteristic of vitrimer systems. Disulfide-containing polymers have been studied both as neat resin systems and as matrices for fiber-reinforced composites [17, 26]. Consequently, dynamic disulfide bonds have been incorporated into various polymer networks, including epoxy resins [34] and polyurethanes [29, 35, 36]. Disulfide-based vitrimers can achieve relatively high glass transition temperatures, with values of up to 187 °C being reported [37].

The resin systems investigated in this study are epoxy polymers containing dynamic disulfide bonds, which allow the material to undergo reversible exchange reactions. In addition to thermal activation, disulfide bonds can also be cleaved through UV irradiation, while the presence of a catalyst can further facilitate this process.

Dynamic covalent disulfide bonds offer a combination of material robustness and reversibility. Vitrimer materials are characterized by several advantageous properties, including structural rigidity, good mechanical performance, chemical stability, reprocessability, and relatively facile degradation. These characteristics make vitrimers promising candidates for novel applications and closed-loop material cycles, thereby contributing to more sustainable material systems.

The development of vitrimer systems generally involves a trade-off between glass transition temperature, mechanical properties, chemical resistance, and the temperature required for healing or reprocessing. A higher elastic modulus is typically associated with a higher glass transition temperature, which consequently leads to an increased healing temperature. The relationship between healing temperature and elastic modulus for various self-healing materials is presented in Figure 1-4 [26]. Sulfur-based chemistry offers a broad range of possibilities, making disulfide bonds particularly attractive for the development of self-healing materials [27].

1.2.4. Epoxy-Based Vitrimers

Epoxy resins remain the most widely adopted platform for vitrimer development, owing to the maturity of epoxy chemistry, the broad commercial availability of epoxy monomers and curing agents, and the direct compatibility of vitrimer exchange chemistries with established epoxy formulation and processing routes. Conventional epoxy vitrimers are typically formulated using diglycidyl ether of bisphenol A (DGEBA) as the base resin, cured with an amine or anhydride hardener that has been functionalized to incorporate the desired exchangeable bond, most commonly transesterification catalysts, aromatic disulfides, or imine-forming aldehydes. This formulation flexibility has allowed researchers to tune the resulting network's glass transition temperature, crosslink density, and exchange kinetics largely independently of one another, by varying the epoxy backbone, the hardener structure, and the stoichiometric ratio between them.

Growing attention has also been directed toward reducing the fossil-based content of epoxy vitrimer formulations, motivated by the same sustainability concerns that originally drove interest in vitrimers as a recyclable alternative to conventional thermosets. Biobased epoxy monomers derived from renewable feedstocks, such as vanillin obtained from lignin, have been developed as replacements for DGEBA, allowing the exchangeable functionality itself to be built directly into the epoxy monomer rather than introduced solely through the hardener. This monomer-level integration of dynamic chemistry offers an important practical advantage: because the exchangeable groups are already present in the epoxy component, any curing agent suitable for standard epoxy-amine chemistry can, in principle, be used to obtain a functioning vitrimer, considerably broadening the range of achievable network architectures and mechanical properties.

Epoxy vitrimers formulated with aromatic disulfide hardeners, including the CIDETEC-patented system used in this study, have been reported to achieve glass transition temperatures in the range of approximately 85 to 135 °C alongside stress relaxation times on the order of seconds to minutes at processing temperatures, representing a favorable combination of thermoset-like performance and vitrimer-like reprocessability that is difficult to achieve with alternative exchange chemistries. However, this same aromatic disulfide functionality, along with imine linkages where present, introduces a thermal stability ceiling somewhat below that of conventional amine-cured epoxy thermosets, since the exchangeable

bonds themselves are typically among the first structural features to undergo thermal decomposition at elevated temperature. This inherent trade-off between reprocessability and thermal stability becomes especially consequential during the curing and reprocessing stages, where the elevated temperatures required to activate the desired exchange behavior simultaneously place the network at risk of irreversible thermal degradation, a tension examined in detail in the following section.

1.2.5. Processing and Reprocessing of Vitrimers: The Role of Thermal Degradation

Successfully processing an epoxy vitrimer requires navigating a delicate balance between achieving full cure and avoiding thermal degradation of the network. Due to the exothermic nature of the curing reaction, the internal temperature of a curing sample can rise significantly above the nominal processing temperature, particularly at high heating rates or in thick sections where heat dissipation is limited. If this overheating exceeds a critical threshold, the reaction kinetics can accelerate uncontrollably in a self-sustaining process known as thermal runaway, driving the sample temperature well above the resin's degradation onset and causing irreversible damage to the cured network. Even without reaching full thermal runaway, curing at temperatures close to the degradation threshold can produce partial, localized degradation that compromises the resulting material's properties without necessarily being visually apparent.

This challenge is compounded during reprocessing, since vitrimers must typically be heated above both their glass transition temperature and their topology freezing transition temperature to activate the bond exchange reactions responsible for reshaping and stress relaxation. At these elevated temperatures, however, the same thermal energy that drives the desired topological rearrangement also accelerates competing degradation pathways within the network, meaning that the reprocessing window is fundamentally constrained by the material's thermal stability rather than by the exchange kinetics alone. For vitrimers based on aromatic disulfide, this constraint is particularly relevant, as the exchangeable bonds that enable reprocessability are frequently among the first structural features to decompose under prolonged or excessive heating.

To address this challenge, time-temperature-transformation (TTT) diagrams have been developed as a practical tool for identifying safe processing and reprocessing conditions [1,

38]. By overlaying the kinetics of curing, or, for reprocessing, the kinetics of the exchange reaction, with the kinetics of thermal degradation on a single time-temperature plot, these diagrams allow the maximum processing temperature and minimum required processing time to be identified for a given target degree of cure or reshaping, while remaining below a specified tolerable degradation threshold. This approach has been successfully applied to characterize both the processing and reprocessing windows of the aromatic disulfide-based vitrimer examined in this dissertation, using isoconversional kinetic analysis of thermogravimetric data to predict degradation behavior under arbitrary time-temperature histories. However, while these TTT diagrams establish the time-temperature boundaries within which degradation remains below a chosen numerical threshold, they do not, on their own, quantify how a given degree of degradation actually translates into a corresponding change in the material's physical and mechanical properties, a question addressed in the following section.

1.2.6. Self-healing and reshaping properties

Self-healing in polymeric materials refers to the ability of a material to recover part or all of its properties after damage without requiring complete replacement of the damaged component. In conventional thermosetting polymers, permanent covalent cross-links restrict molecular mobility after curing, meaning that cracks or other forms of damage cannot readily be repaired through molecular rearrangement. In vitrimeric materials, however, the presence of dynamic covalent bonds provides an alternative mechanism for damage recovery. When the material is exposed to appropriate thermal or other activation conditions, these dynamic bonds can undergo exchange reactions, allowing the polymer network to rearrange and establish new connections across damaged regions. In this context, self-healing is therefore closely related to the same bond-exchange processes that give vitrimers their stress-relaxation and reprocessing capabilities [12, 39].

Healing behavior has been reported for thermoset vitrimers, including photo-weldable epoxy/carbon-nanotube composite vitrimeric materials, in which the healing process is enabled by transesterification reactions between diepoxy and dicarboxylic acid functionalities [40]. The combination of shape memory-properties is also attractive. Thus graphene-based

dual triggered shape memory vitrimer nano composites were reported with transesterification chemistry [41].

Several studies reported in the literature have demonstrated the reparability and self-healing capabilities of disulfide-containing materials. De Luzuriaga et al. demonstrated the reparability of vitrimer-based carbon-fiber-reinforced polymers (CFRPs) by stacking several thin, cured vitrimer CFRP sheets and subsequently hot-pressing them to produce a single multilayered CFRP sheet [17]. In their study, 4-Aminophenyl disulfide (APhD) was employed as the hardener for the epoxy monomers. Furthermore, previously tested and delaminated interlaminar shear strength (ILSS) specimens were successfully repaired by hot-pressing at 200 °C and 100 bar for 5 min. A comparison of the mechanical strength of pristine and repaired specimens confirmed the effective recovery of the material properties. In a further experiment, fully cured specimens were ground into smaller pieces and subsequently hot-pressed to form new sheets, demonstrating the reprocessability of the material [17].

Lei et al. investigated the self-healing behavior of cross-linked aliphatic disulfide-containing polymers prepared using Thioplast EPS25 [30]. The healing process was performed at room temperature under alkaline conditions using diazabicycloundecene (DBU) and tributylphosphine (TBP) as a catalyst. Initially, a polymer specimen was fractured into two separate pieces. After 24 h of healing at room temperature, the tensile strength was restored with a healing efficiency of 91%. In the absence of TBP, the healing efficiency decreased to only 13%, which was attributed to the contribution of dangling polymer chains and hydrogen bonding. In contrast, control specimens without disulfide bonds exhibited no significant healing. Increasing the temperature to 60 °C considerably accelerated the disulfide-exchange reaction, reducing the required healing time to approximately 2 h.

The ability of the material to undergo multiple healing cycles was also demonstrated through repeated healing experiments. Furthermore, the reaction was shown to be insensitive to exposure to air, as the two fractured pieces could be separated for a certain period before being recombined without significantly affecting the healing process. In addition to self-healing, the material exhibited reprocessability. A cylindrical specimen was compressed and successfully remolded into a flat geometry after 48 h at room temperature. Similarly, chopped polymer material could be compressed and reshaped into a flat geometry. However, the occurrence of disulfide exchange and self-healing at room temperature was also associated with significant creep behavior [42].

The wide range of available disulfide-containing monomers enables the design of various cross-linked polymer networks with tailored properties. Takahashi et al. synthesized a novel disulfide-containing component in which the disulfide groups are incorporated directly into a diepoxide monomer, bis(4-glycidyloxyphenyl)disulfide (BGPDS) [43]. In contrast to the studies described above, their work investigated the degradation behavior of disulfide-containing epoxy thermosets through a disulfide-exchange mechanism rather than a thiol–disulfide exchange reaction. For this purpose, diphenyl disulfide (DPDS) was employed as the exchange partner [42].

1.2.7. Effects of Thermal Degradation on Physical and Mechanical Properties

Beyond the kinetic characterization of degradation onset and rate, a separate body of literature has examined how exposure to elevated processing or aging temperatures translates into measurable changes in the physical and mechanical properties of epoxy resins and epoxy-based composites [44-46]. These studies have generally approached the problem from a practical processing perspective, correlating the imposed thermal history—such as peak temperature, exposure temperature, and treatment duration—with subsequent changes in properties such as glass transition temperature, stiffness, strength, and interlaminar shear strength [44, 46]. However, the resulting property changes are typically expressed as functions of the applied temperature–time history rather than being directly correlated with an independently quantified degree of thermal degradation.

In fiber-reinforced epoxy laminates, curing-induced overheating has been shown to produce measurable losses in interlaminar shear strength. Sorrentino et al. reported reductions of up to approximately 13% as the magnitude of the temperature peak increased during curing, demonstrating that excessive exothermic heating can adversely affect matrix-dominated mechanical properties [44]. Similar sensitivity to thermal history has been observed in epoxy adhesives, where variations in cure and post-cure temperature have been shown to modify the glass transition temperature, T_g, Young's modulus, yield strength, and failure strain [46, 47]. At sufficiently severe thermal conditions, reductions in stiffness and strength and changes in T_g have been observed, indicating that excessive thermal exposure can alter both the mechanical response and the underlying network structure. More generally, thermal aging studies of epoxy networks have demonstrated that prolonged exposure at elevated

temperatures can reduce T_g, strain-to-failure, and mechanical performance as irreversible degradation progresses [46, 48].

However, the majority of this prior work characterizes property loss as a function of processing temperature and exposure time directly, without first quantifying the corresponding degree of thermal degradation using an independent, mass-loss-based metric such as thermogravimetric analysis. As a result, while it is well established that excessive thermal exposure degrades mechanical and thermal properties in epoxy resins broadly, a direct, quantitative correlation between a measured degree of degradation and the resulting evolution of glass transition temperature and viscoelastic behavior, specifically for epoxy-based vitrimers, has not yet been systematically characterized over a controlled range of degradation levels and correlated with both thermal and viscoelastic properties in the literature. This distinction, between characterizing degradation by processing conditions versus by an independently measured degree of degradation, forms the basis of the research gap addressed in this dissertation, outlined explicitly in the following section.

1.2.8. Research Gap

The literature reviewed in the preceding sections establishes three separate bodies of knowledge that, together, define the boundaries of what is currently understood about thermal degradation in epoxy vitrimers, while also revealing where these bodies of knowledge fail to connect. First, the thermal degradation kinetics of aromatic disulfide-based epoxy vitrimers have been characterized in detail using isoconversional analysis, and this kinetic framework has been successfully applied to construct processing and reprocessing maps that identify safe time-temperature windows for curing and reshaping. Second, the effect of elevated processing temperatures on the mechanical and thermal properties of epoxy resins has been documented, showing that overheating during cure or post-cure treatment can measurably reduce glass transition temperature, modulus, and strength. Third, the vitrimer concept itself, and its exchange chemistries, and reprocessing behavior, has been extensively characterized from a materials-design perspective.

What remains absent from this literature is a direct, quantitative link between these three areas, specifically, a correlation established between an independently measured degree of thermal degradation, determined through mass-loss-based kinetic analysis rather than

inferred from processing conditions alone, and the corresponding evolution of glass transition temperature and viscoelastic properties in an epoxy vitrimer. Existing processing and reprocessing maps define the time-temperature conditions under which a chosen degradation threshold is not exceeded, but they do not, on their own, indicate how the material's physical performance actually changes once that threshold is approached or crossed. Conversely, studies documenting mechanical property loss under thermal exposure generally characterize degradation by processing history rather than by a quantified degree of degradation, making it difficult to generalize their findings to arbitrary time-temperature profiles or to other formulations.

This dissertation addresses this gap by establishing that missing correlation for an aromatic disulfide-containing epoxy vitrimer, quantifying the degree of thermal degradation through thermogravimetric analysis and Friedman isoconversional kinetics, and directly relating this quantified degradation to the resulting evolution of glass transition temperature and viscoelastic behavior, measured through DSC and DMA respectively. In doing so, this work extends existing degradation-prediction tools from a purely kinetic framework into one capable of anticipating the actual physical and mechanical consequences of thermal exposure, providing a more complete basis for the safe design of processing and reprocessing conditions for this class of materials.

2. MATERIALS AND METHODS

2.1. Materials

The epoxy vitrimer studied in this work consists of commercially available functional epoxy groups DGEBA (Araldite LY1564) and a new (also commercially available) hardener with dynamic cross-linking based on aromatic disulfide species (4-Aminophenyl disulfide). For the mixing, the NH equivalents were set as 1.1 per epoxy group.

2.2. Formulation and Curing Process

The epoxy–hardener formulation was prepared in a mass ratio of 1:0.29 (epoxy monomer:hardener), corresponding to 0.29 g of 4-Aminophenyl disulfide per gram of Araldite LY1564. The two components were weighed into a beaker and mixed at 100 °C under nonstop stirring until a homogeneous mixture was obtained as instructed by CIDETEC, who hold a patent for this formulation.

The homogeneous formulation was then poured into a preheated custom-made glass mold and cured in an oven according to the following two-stage schedule: 1 h at 140 °C, followed by 4 h at 160 °C. After curing, samples were allowed to cool to room temperature and were demolded and prepared coupon to the desired dimensions prior to testing.

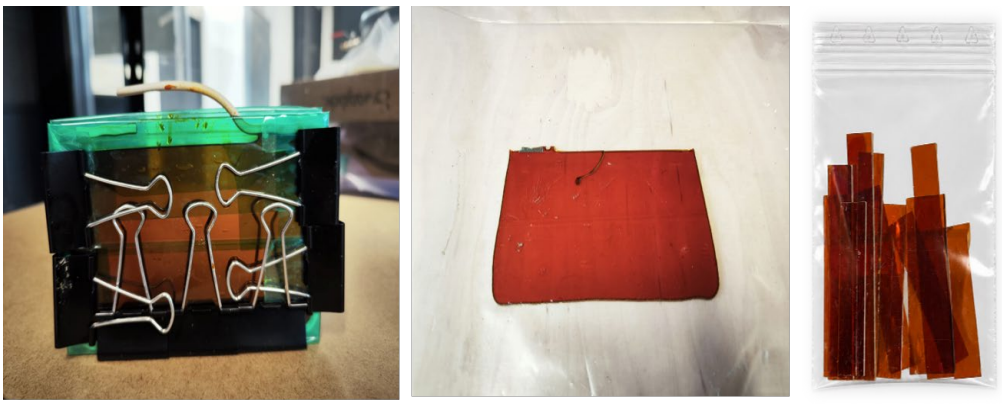


Figure 2-1 Curing and sample preparation process of the epoxy-based vitrimer resin, including formulation, curing, demolding, and preparation of specimens for characterization

Rectangular plate specimens were prepared for dynamic mechanical analysis (DMA), with required dimensions, consistent with prior characterization of this vitrimer system (Figure 2-1).

2.3. Isoconversional Kinetic Analysis

Thermal analysis (TA) techniques allow a material property to be tracked while a sample is subjected to a controlled temperature program, making them well suited to characterizing the kinetics of thermally driven processes. In this work, the kinetics of thermal degradation was analyzed using this general approach, applied to DMA and TGA data, respectively, and processed through Friedman's isoconversional method [49].

2.3.1. Defining the extent of transformation from DMA and TGA data

Dynamic mechanical analysis (DMA) was used for two different purposes and therefore employed different testing configurations. The viscoelastic properties of the pristine and thermally degraded specimens were characterized by temperature-sweep measurements in a dual (double)-cantilever configuration. In this mode, the rectangular specimen is fixed at both ends while a central movable clamp applies an oscillatory displacement perpendicular to its length, producing a symmetric bending deformation. The resulting force response is phase-shifted relative to the applied displacement by the phase angle, δ, from which the storage modulus, E', loss modulus, E'', and $\tan\delta$ are determined as functions of temperature.

In contrast, the isothermal stress-relaxation experiments used for the kinetic analysis were performed in tensile mode. In these tests, the specimen was subjected to a prescribed tensile deformation and the decrease in stress with time was recorded at constant temperature. The resulting normalized stress-relaxation curves were subsequently used to define the degree of relaxation, α, and to determine the corresponding kinetics using Friedman's isoconversional method.

Reprocessing of vitrimers is governed by the exchange reactions occurring between their dynamic bonds, which macroscopically result in stress relaxation under a fixed applied strain. During the isothermal tensile stress-relaxation experiments, the applied strain was maintained constant while the stress, $\sigma(t)$, progressively decreased with time as the network

rearranged. The corresponding stress-relaxation modulus was obtained from the measured stress response at constant strain. For the isoconversional kinetic analysis, the progress of stress relaxation was expressed through the degree of relaxation, α. The initial state corresponds to $\alpha = 0$, whereas $\alpha = 1$represents complete stress relaxation. Accordingly, using the normalized stress response, the degree of relaxation can be expressed as:

$$\alpha\,(t) = \frac{\sigma_0 - \sigma\,(t)}{\sigma_0} \qquad 2.1$$

where, σ_0 is the initial stress immediately after application of the prescribed strain and $\sigma(t)$is the stress remaining at time t. This definition allows the stress-relaxation response to be treated as a transformation process and subsequently analyzed using Friedman's isoconversional method.

Thermogravimetric Analysis (TGA) is a thermal analysis technique that monitors the mass of a sample as it is subjected to a controlled temperature program under a defined atmosphere. The sample is placed in a pan suspended from a highly sensitive microbalance inside a furnace, while a purge gas typically nitrogen or air flows continuously through the chamber. As the temperature increases at a constant heating rate, any mass loss resulting from moisture evaporation, volatilization, or thermal decomposition is recorded in real time, producing a thermogram of normalized mass (%) as a function of temperature. Because thermal degradation is a kinetically activated process, TGA experiments performed at several different heating rates reveal a systematic shift of the mass-loss curve toward higher temperatures with increasing heating rate, providing the multi-rate dataset required for isoconversional kinetic analysis. In this study, TGA was used to characterize the thermal degradation behavior of the fully cured vitrimer and to generate the kinetic data underlying the Friedman isoconversional analysis and the resulting degradation-prediction map.

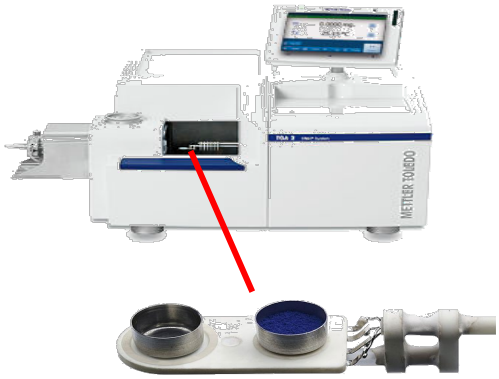


Figure 2-2 Schematic representation of the thermogravimetric analysis (TGA) principle used to characterize the thermal degradation behavior of the cured vitrimer resin

For the degradation process, TGA monitors the evolving sample mass, and the degree of degradation is assumed to scale linearly with mass loss:

$$\alpha(t) = \frac{m_i - m(t)}{m_i - m_f} \qquad 2.2$$

where m_i and m_f are the initial and final sample masses, respectively.

2.3.2. The isoconversional hypothesis

Isoconversional methods rest on the assumption that, at a fixed degree of conversion α, the transformation rate depends only on temperature:

$$\left[\frac{d\ln\left(\frac{d\alpha}{dt}\right)}{dT^{-1}}\right]_{\alpha} = \frac{E_\alpha}{R} \qquad 2.3$$

where T is the temperature, R is the universal gas constant, and Eα is the apparent activation energy at that particular degree of conversion. In most real thermally activated processes, the underlying energy barrier stays roughly constant as the reaction proceeds. When the transformation is more complex, involving several superimposed sub-processes with different activation energies, or processes that deviate from simple Arrhenius behavior, Eα varies with α. For this reason, Eα should be understood as an apparent activation energy rather than a fixed, mechanistic one.

2.3.3. The rate equation and Friedman's linearization

Integrating (2.3) gives the general rate expression:

$$\frac{d\alpha}{dt} = A_\alpha f(\alpha) \exp(-\frac{E_\alpha}{RT}) \qquad 2.4$$

so that, at a given conversion, the reaction rate is fully described by two parameters: the apparent activation energy Eα and the term Aαf(α). The goal of the isoconversional analysis is to extract both parameters as functions of α.

To do this, the degree of transformation is discretized into small, equally spaced steps, $\alpha_j = j\Delta\alpha$, and a series of experiments is performed at different heating rates $\beta \equiv dT/dt$ (non-isothermal tests) or at fixed temperatures (isothermal tests). Friedman's differential isoconversional method linearizes (2.4) directly:

$$\ln\left(\frac{d\alpha}{dt}\right)_{i,j} = \frac{E_j}{RT_{j,i}} + \ln[Af(\alpha)]_j \qquad 2.5$$

Here the subscript *i* denotes a particular experiment (heating rate β_i for non-isothermal runs, or temperature T_i for isothermal runs), and the subscript *j* denotes a fixed degree of transformation α_j. For each heating rate, the transformation rate $d\alpha/dt|_{j,i}$ and its corresponding temperature $T_{j,i}$ are extracted at each α_j. Plotting $\ln(d\alpha/dt)_{j,i}$ against the reciprocal temperature $1/T_{j,i}$ should yield a straight line, whose slope and intercept give E_j and $Af(\alpha)|_j$ respectively.

2.3.4. Predicting isothermal behavior from the extracted kinetic parameters

Once E_j and $Af(\alpha)|_j$ are known across the full range of α, (2.4) can be integrated to predict how long it takes to reach a target conversion under isothermal conditions:

$$\Delta t = \int_{\alpha_m}^{\alpha_{m+n}} \frac{\exp(\frac{E_\alpha}{RT})}{Af(\alpha)}\, d\alpha \qquad 2.6$$

where T is the constant (isothermal) temperature, Δt is the time needed to go from conversion α_m to α_{m+n}, and $\alpha_{m+n} - \alpha_m = n\Delta\alpha$ follows the same discretization used to obtain the kinetic parameters. Since this integral is evaluated at equally spaced α values, it was computed using the closed Newton–Cotes Bode's formula (n = 5) [50].

2.3.5. Extending the prediction to arbitrary (non-isothermal) temperature profiles

To predict degradation under the actual, non-isothermal conditions of the oven treatments, the Roduit method can be adapted following Farjas and Roura [51, 52]. Here, the temperature history is discretized into a series of small, constant time intervals Δt_k, with $T_k = T(t_k)$. (2.4) is then summed stepwise over these intervals:

$$\alpha_{k+1} = \alpha_k + Af(\alpha)|_k \,.\exp(-\frac{E_k}{RT_k})\,\Delta t_k \qquad 2.7$$

where α_k, E_k, and $Af(\alpha)|_k$ are, respectively, the conversion, apparent activation energy, and pre-exponential term at temperature T_k, and Δt_k is the time step between T_k and T_{k+1}. Starting from $\alpha_o = 0$ at k = 0, this iterative scheme yields the predicted time evolution of the degree of transformation (curing or degradation) for any temperature program including the isothermal oven dwells at 220 °C used to generate the controlled degradation states examined in this work.

2.4. Methods

2.4.1. Thermogravimetric Analysis (TGA)

The thermal stability of the cured samples was studied by thermogravimetric analysis (TGA). Experiments were performed under a flow of air at 50 mL·min^{-1}. Pieces of fully cured samples of a mass of approximately 5–8 mg were degraded between 50 and 800 °C at a series of constant heating rates (e.g., 1.25, 2.5, 5, 10, and 20 °C·min^{-1}) to support the Friedman isoconversional kinetic analysis described in Section 2.3. The thermal stability was additionally studied in isothermal mode to confirm baseline stability of the pristine (undegraded) resin prior to the controlled degradation treatments described below.

2.4.2. Controlled Thermal Degradation (Oven Treatment)

To generate specimens with defined, controlled degrees of thermal degradation, fully cured samples were subjected to isothermal dwelling in a convection oven at a constant temperature of 220 °C for dwell times of 30 min, 1 h, 2 h, and 4 h. This target temperature and the corresponding dwell times were selected using the degradation prediction map

derived from the isoconversional kinetic analysis (Section 2.4), so as to span a representative range of degradation states from mild, near-onset degradation to more advanced degradation while remaining within the regime where the vitrimer retains structural integrity for mechanical testing. After each treatment, samples were removed from the oven and allowed to cool to room temperature under ambient conditions before further characterization. The mass of each specimen was recorded before and after treatment to quantify the corresponding degree of degradation (α), consistent with the mass-loss-based definition used in the isoconversional analysis.

2.4.3. Dynamic Mechanical Analysis (DMA)

Dynamic mechanical analysis (DMA) was used both to characterize the stress-relaxation behavior of the pristine epoxy vitrimer and to evaluate the influence of thermal degradation on its viscoelastic properties. These two objectives were investigated using different experimental configurations.

Tensile stress-relaxation experiments were performed by CIDETEC using a DMA Q800 instrument in tensile mode. The specimens were initially subjected to a preload of 1×10^{-3}N to maintain straightness. After reaching the selected testing temperature, the samples were held for an additional 30 min to ensure thermal equilibrium. A tensile strain of 1% was then applied and maintained constant throughout the experiment, while the resulting decrease in stress with time was recorded. The corresponding stress-relaxation modulus was subsequently calculated and used for the isoconversional kinetic analysis of the vitrimer relaxation process.

The viscoelastic properties of the pristine and thermally degraded specimens were characterized separately using a Mettler Toledo DMA SDTA861 in double-cantilever configuration. Rectangular specimens of approximately $80 \times 10 \times 2$mm³ were tested at a frequency of 1 Hz during heating from 20 to 200 °C at a constant rate of 5 °C·min^{-1}. The storage modulus, E', loss modulus, E'', and loss factor, $\tan\delta$, were recorded as functions of temperature. The glass transition temperature, T_g, was determined from the temperature corresponding to the maximum of the loss-modulus, E'', peak.

3. RESULTS AND DISCUSSION

3.1. Thermal Degradation Behavior (TGA)

3.1.1. Normalized TGA Curves at Multiple Heating Rates

Figure 3-1 presents the normalized mass curves obtained by thermogravimetric analysis (TGA) of the fully cured epoxy vitrimer at constant heating rates of 1.25, 2.5, 5, 10, and 20 °C·min^{-1}. The measurements provide an initial assessment of the thermal stability and decomposition behavior of the material and, more importantly, generate the multi-heating-rate data required for the subsequent Friedman isoconversional kinetic analysis.

At all heating rates, the specimens retain approximately 100% of their initial mass throughout the low-temperature region, with no substantial mass loss observed up to approximately 250–280 °C. This indicates that the cured vitrimer remains comparatively thermally stable within this temperature range. Above this region, a pronounced decrease in normalized mass is observed, marking the onset of the main thermal degradation process.

The TGA curves reveal a multi-stage degradation behavior rather than a single continuous mass-loss event. The first major mass-loss stage occurs approximately between 270 and 350 °C, during which the normalized mass decreases rapidly from close to 100% to approximately 60%. This is followed by a less pronounced mass-loss region extending approximately from 350 to 450 °C, where the curves exhibit a shoulder and the remaining mass gradually decreases toward approximately 40–50%. A second major degradation stage subsequently occurs at higher temperatures, ultimately resulting in almost complete mass loss. The presence of these distinct regions indicates that the thermal decomposition of the epoxy vitrimer is a complex process involving more than one degradation step rather than a single elementary reaction.

A clear influence of heating rate can be observed throughout the degradation process. As the heating rate increases from 1.25 to 20 °C·min^{-1}, the degradation curves systematically shift toward higher temperatures. This displacement is particularly evident during both the initial mass-loss stage and the final decomposition region. At the lowest heating rate of 1.25

°C·min^{-1}, significant degradation begins at a lower temperature and the final mass-loss stage is completed at approximately 520 °C. In contrast, at 20 °C·min^{-1}, the corresponding degradation events are displaced considerably toward higher temperatures, with near-complete decomposition occurring only above approximately 650 °C.

This heating-rate dependence is characteristic of a kinetically controlled thermal degradation process. At lower heating rates, the specimen is exposed to each temperature interval for a longer period, providing more time for thermally activated degradation reactions to proceed. Consequently, a given degree of degradation can be reached at a comparatively lower temperature. At higher heating rates, the residence time at each temperature is shorter, and the specimen must reach a higher temperature before the same degree of transformation is achieved. Therefore, the observed shift should not be interpreted as an intrinsic increase in the thermal stability of the material with heating rate, but rather as a consequence of the kinetics of the degradation process.

Despite this temperature shift, the overall shape and sequence of the mass-loss regions remain broadly comparable across the five heating rates. In particular, all curves exhibit an initial major mass-loss event, an intermediate shoulder, and a subsequent higher-temperature decomposition stage. This similarity suggests that the same overall degradation processes occur throughout the investigated heating-rate range, while their apparent temperatures are displaced according to the imposed thermal history.

The systematic displacement of the TGA curves is particularly important for the kinetic analysis performed in the following section. At any selected degree of degradation, (α), each heating rate reaches that conversion at a different temperature and with a different transformation rate. These differences provide the information required by Friedman's differential isoconversional method to determine the apparent activation energy, ($E\alpha$), independently at successive degrees of degradation. Consequently, rather than characterizing the thermal stability of the vitrimer using only a single degradation-onset temperature, the multi-rate TGA dataset enables the evolution of the degradation kinetics throughout the transformation to be quantified.

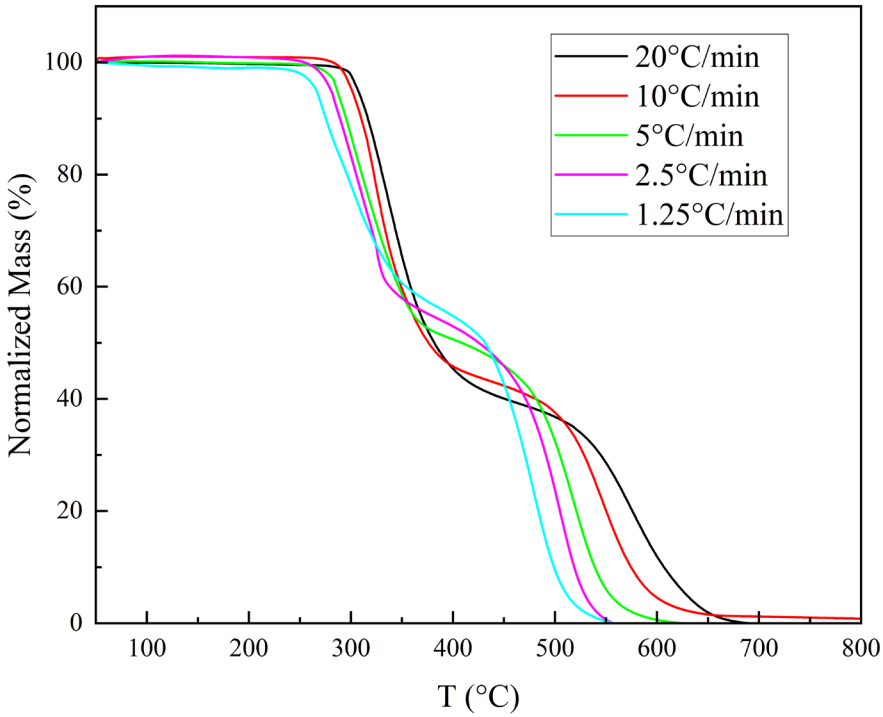


Figure 3-1 Normalized mass-loss curves of the cured epoxy vitrimer obtained by TGA at different heating rates (1.25, 2.5, 5, 10, and 20 °C/min)

3.2. Isoconversional Kinetic Analysis of Degradation

3.2.1. Friedman Analysis: Apparent Activation Energy vs. Degree of Degradation

Figure 3-2 presents the apparent activation energy, (Eα), obtained from Friedman's differential isoconversional analysis as a function of the degree of thermal degradation, (α), together with the correlation coefficient of the corresponding linear regressions. The results show that the apparent activation energy is not constant throughout the degradation process, indicating that the thermal decomposition of the epoxy vitrimer cannot be adequately represented by a single activation energy over the investigated conversion range.

At very low degrees of degradation, approximately ($\alpha < 0.01$), (Eα) exhibits pronounced fluctuations, with values ranging from approximately 60 to 160 $kJ \cdot mol^{-1}$. The correlation coefficient is also noticeably lower in this initial region, particularly at the first conversion points. This behavior is most likely associated with the difficulty of accurately determining degradation rates close to the onset of mass loss. At such low conversion levels, the absolute change in sample mass is very small, making the numerical determination of ($d\alpha/dt$)

particularly sensitive to experimental noise and data-processing uncertainties. Consequently, the activation-energy values obtained in this initial region should be interpreted with caution. Once the degree of degradation exceeds approximately (α = 0.01), the Friedman regressions become considerably more stable, with correlation coefficients remaining close to unity over almost the entire remaining conversion range. In parallel, (Eα) increases toward approximately 200 $kJ \cdot mol^{-1}$ and remains relatively stable between approximately (α = 0.015) and 0.04. The presence of this broad plateau suggests that the degradation process within this conversion interval is governed by a comparatively consistent effective kinetic barrier.

Beyond approximately (α = 0.04), the apparent activation energy begins to decrease progressively. (Eα) falls from approximately 200 $kJ \cdot mol^{-1}$ to around 170–175 $kJ \cdot mol^{-1}$ between (α= 0.05) and 0.065, followed by a more pronounced local minimum near (α= 0.07), where a value of approximately 150 $kJ \cdot mol^{-1}$ is obtained. After this minimum, the apparent activation energy recovers and gradually increases toward approximately 185–190 $kJ \cdot mol^{-1}$ as (α) approaches 0.10.

Importantly, the correlation coefficient remains very high throughout most of this region, including the gradual decrease in (Eα). Only a relatively small local reduction in the correlation coefficient accompanies the pronounced minimum near (α= 0.07). Therefore, the overall evolution of (Eα) cannot be attributed simply to poor linear regression. Instead, the conversion dependence of the apparent activation energy indicates that the effective kinetics of degradation evolve as thermal decomposition progresses.

This behavior is consistent with the multi-stage character of the TGA curves presented in Figure 3-1. The normalized mass curves exhibit more than one distinct mass-loss region, while the Friedman analysis independently shows that the effective activation barrier varies with conversion. Taken together, these observations indicate that thermal degradation is kinetically complex and is unlikely to be governed by a single elementary decomposition process throughout the complete transformation. Different degradation reactions may contribute with different relative importance as the network progressively decomposes.

However, the individual regions of the (Eα (α)) curve should not be assigned directly to the cleavage of specific chemical bonds based on the TGA and isoconversional results alone. The present measurements establish changes in the overall degradation kinetics but do not independently identify the chemical species or bonds responsible for each degradation stage. Nevertheless, considering that the studied material consists of a DGEBA-based epoxy network

containing dynamic aromatic disulfide cross-links, the observed variation in apparent activation energy is compatible with progressive changes in the dominant degradation processes as different parts of the cross-linked network become involved.

The conversion dependence of (Eα) also has an important consequence for kinetic prediction. If a single average activation energy were used to represent the entire degradation process, the changes in kinetic behavior observed across the conversion range would be neglected. In the present work, the Friedman isoconversional approach instead provides an apparent activation energy and corresponding kinetic term at each degree of degradation. This allows the degradation rate to evolve with conversion and therefore provides a more appropriate basis for predicting the accumulation of thermal degradation under different time–temperature conditions.

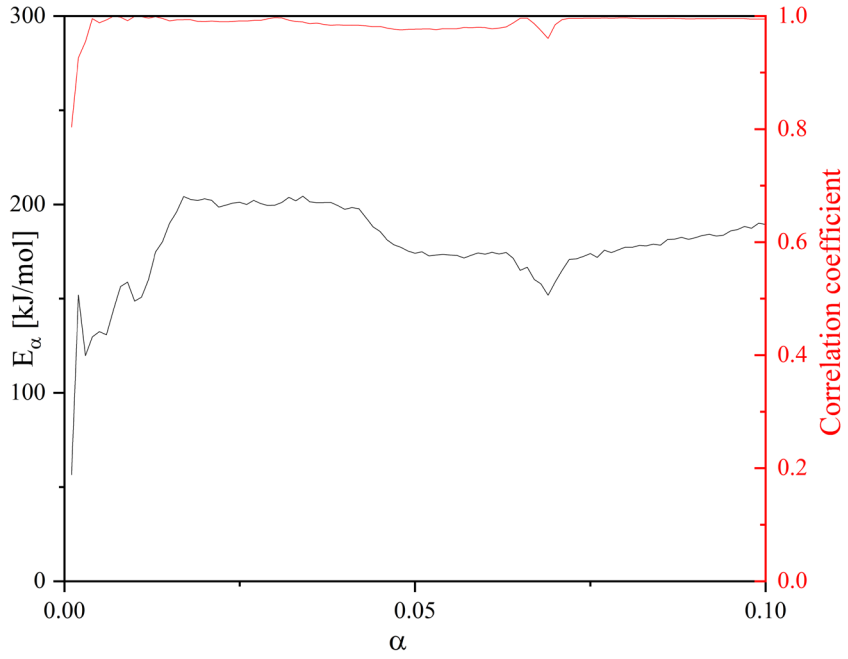


Figure 3-2 Apparent activation energy, (E_α), as a function of the degree of thermal degradation obtained using Friedman's isoconversional analysis

Overall, the results demonstrate that the thermal degradation of the epoxy vitrimer is characterized by a conversion-dependent apparent activation energy. After an uncertain initial region at very low conversion, (Eα) reaches approximately 200 kJ·mol^{-1}, subsequently decreases as degradation progresses, and then partially increases again toward higher conversion. Combined with the consistently high correlation coefficients and the multi-stage TGA response, this evolution supports the treatment of thermal degradation as a kinetically

complex process rather than as a single-step reaction with a constant activation energy. The resulting conversion-dependent kinetic parameters are therefore used in the following sections to predict the thermal degradation behavior and to construct the degradation contours incorporated into the time–temperature–transformation (TTT) diagram.

3.3. Dynamic Mechanical Analysis of Pristine and Degraded Specimens

3.3.1. DMA Friedman/Isoconversional Analysis

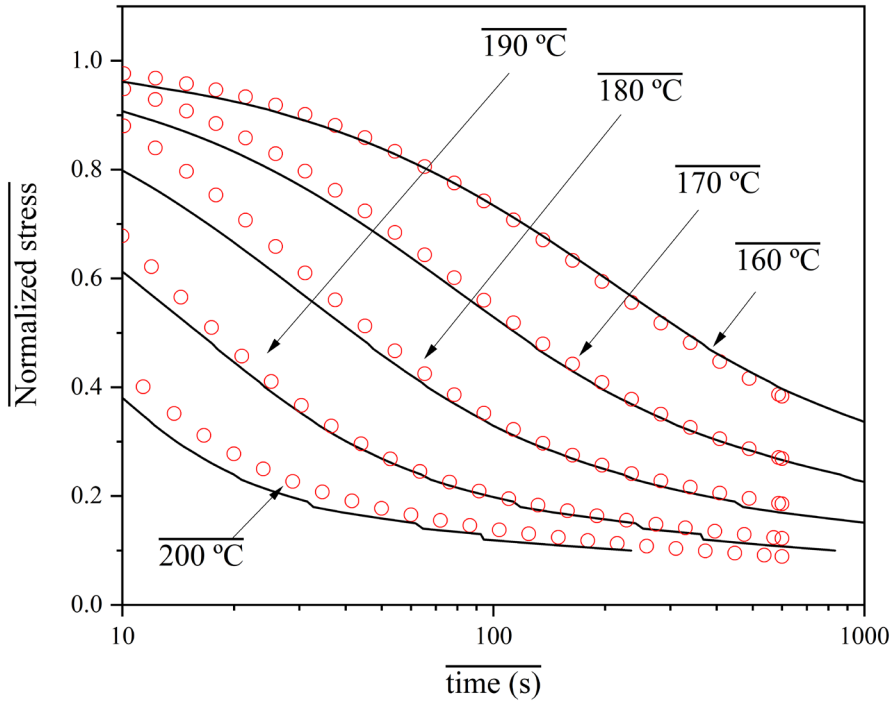


Figure 3-3 Comparison between experimentally measured and isoconversionally predicted stress-relaxation behavior of the pristine epoxy vitrimer at temperatures above the glass transition region

The stress-relaxation behavior of the pristine epoxy vitrimer was investigated by DMA under isothermal conditions in order to characterize the kinetics of the dynamic bond-exchange process. The experimental normalized stress-relaxation curves were analyzed using Friedman's isoconversional method, following the procedure described in Section 2.3. In this approach, the progress of stress relaxation is expressed through the degree of conversion, (α), and the kinetic parameters are determined independently at successive conversion levels. This allows the relaxation process to be described without assuming a single constant activation energy over the entire transformation.

Figure 3-3 compares the experimentally measured normalized stress, represented by the red symbols, with the stress-relaxation curves predicted from the isoconversional kinetic analysis for temperatures between 160 and 200 °C. A strong temperature dependence is clearly observed. Increasing the temperature produces a pronounced shift of the relaxation curves toward shorter times, demonstrating the thermally activated nature of the dynamic exchange process. At 200 °C, a substantial fraction of the initial stress is relaxed within only a few tens of seconds, whereas progressively longer times are required at 190, 180, 170, and 160 °C. This behavior is consistent with accelerated dynamic bond exchange and increased network mobility at higher temperatures.

The conversion dependence of the relaxation kinetics is further illustrated in Figure 3-4, which presents the apparent activation energy, (Eα, obtained from Friedman's analysis as a function of the degree of stress relaxation. The corresponding correlation coefficient remains close to unity over most of the investigated conversion range, generally between approximately 0.98 and 1.00. This high correlation supports the applicability of the Friedman linearization to the stress-relaxation data within the temperature range used for the kinetic analysis.

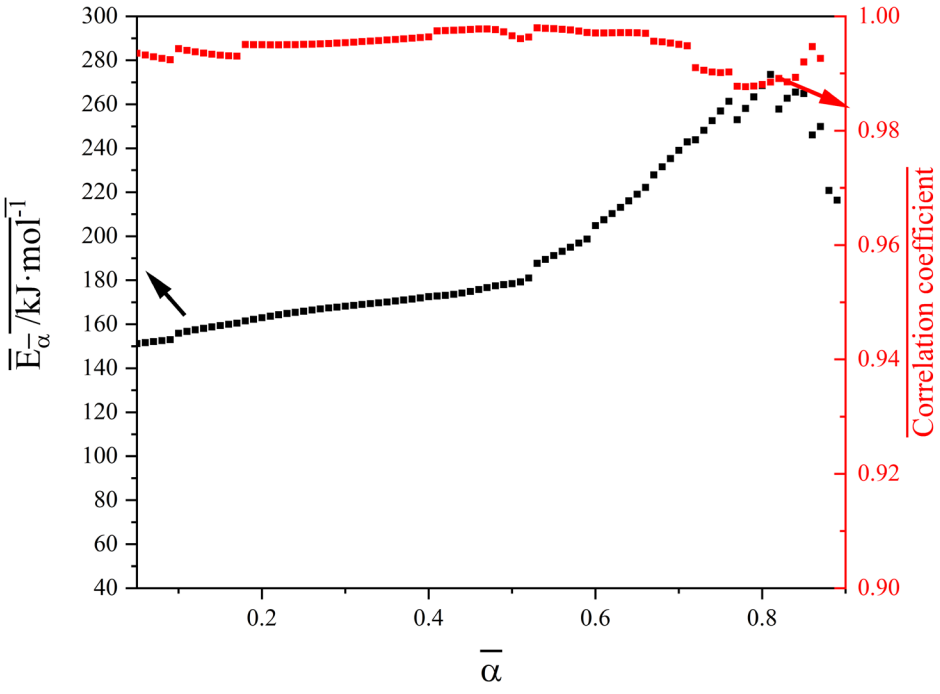
The apparent activation energy is clearly not constant during stress relaxation. At low conversion, (Eα) is approximately 150 $kJ \cdot mol^{-1}$ and initially increases gradually, reaching approximately 170–180 $kJ \cdot mol^{-1}$ by ($\alpha \approx 0.5$). Beyond this region, a much stronger increase is observed, with (Eα) rising to approximately 220 $kJ \cdot mol^{-1}$ around ($\alpha \approx 0.65$) and reaching a maximum of approximately 265–270 $kJ \cdot mol^{-1}$ at ($\alpha \approx 0.8$). Some fluctuations occur at the highest conversion values, where the remaining stress becomes small and the kinetic parameters are consequently more sensitive to experimental uncertainty.

The progressive increase in (Eα) indicates that the effective energy barrier associated with continued stress relaxation becomes larger as the transformation proceeds. In other words, the early stages of network relaxation are kinetically more accessible, whereas achieving increasingly high degrees of relaxation requires overcoming a larger apparent energy barrier. This behavior is consistent with the shape of the experimental relaxation curves: stress decreases comparatively rapidly during the initial stages but progressively approaches a slower relaxation regime at longer times.

The conversion dependence of (Eα) also demonstrates that the stress-relaxation process cannot be adequately represented by a single activation energy or a single characteristic relaxation time over the complete transformation. The dynamic response of the vitrimer is

therefore more complex than a simple single-process Arrhenius relaxation. As the network rearranges, the local molecular environment and constraints surrounding the remaining exchangeable bonds may evolve, resulting in a conversion-dependent effective kinetic barrier. Accordingly, (Eα) should be interpreted as an apparent activation energy describing the overall relaxation process at a given conversion, rather than as the activation energy of an individual disulfide-exchange reaction.

It is also important to distinguish the increase in apparent activation energy from the relaxation rate itself. Within the Friedman framework, the instantaneous rate depends not only on (Eα), but also on the conversion-dependent kinetic term. The increasing (Eα) therefore should not, by itself, be interpreted as direct proof of a continuously decreasing reaction rate. Instead, it demonstrates that the kinetic barrier associated with further network relaxation becomes progressively greater as conversion increases, consistent with the experimentally observed slowing of the approach toward complete stress relaxation.



3-4 Apparent activation energy, (Eα), of the stress-relaxation process and corresponding Friedman correlation coefficient as a function of the degree of conversion

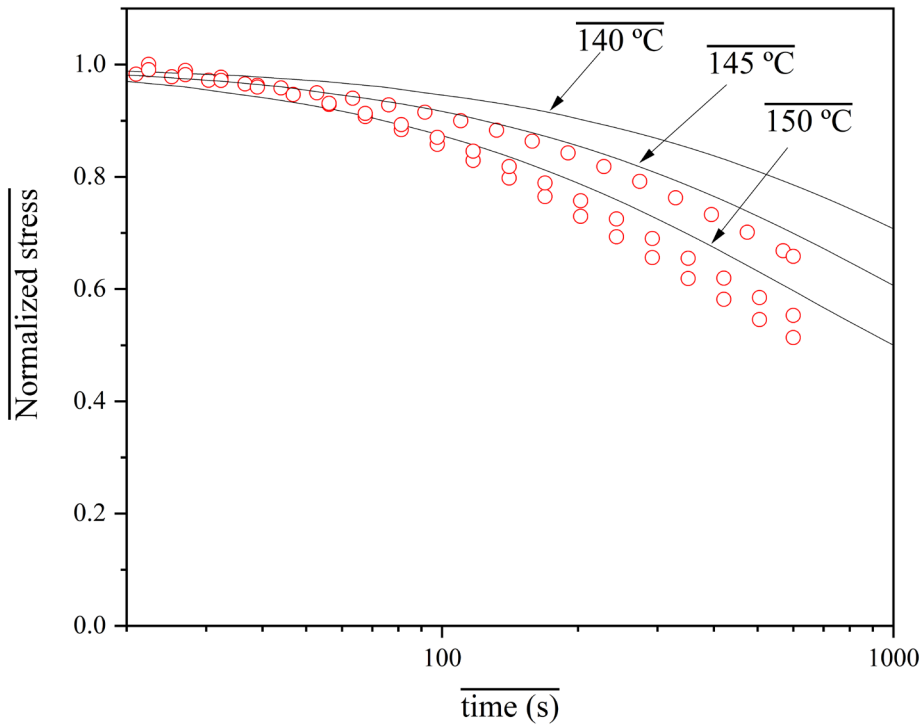


Figure 3-5 Comparison between experimentally measured and isoconversionally predicted stress-relaxation behavior of the pristine epoxy vitrimer at temperatures close to the glass transition region

For this temperature range, which lies sufficiently above the glass transition region of the material, the isoconversional predictions reproduce the experimental relaxation behavior reasonably well. In particular, the model captures both the systematic acceleration of relaxation with increasing temperature and the general shape of the stress decay as relaxation progresses. The agreement indicates that, once sufficient segmental mobility is available, the stress-relaxation process can be satisfactorily represented by the temperature-dependent kinetic framework used in the Friedman analysis.

A different behavior is observed at the lower temperatures of 140, 145, and 150 °C, as shown in Figure 3-5. In this region, the predicted curves increasingly deviate from the experimental measurements. The experimental specimens relax more rapidly than predicted by the extrapolated isoconversional model, and the discrepancy becomes particularly evident as the relaxation proceeds. Therefore, although the model provides a satisfactory representation at higher temperatures, its predictive capability deteriorates when the temperature approaches the glass transition region.

This deviation can be associated with the increasing influence of the glass transition on polymer-chain mobility. The isoconversional treatment assumes that, at a fixed conversion, the temperature dependence of the relaxation rate can be represented through an Arrhenius-

type relationship. This description is more appropriate when the material is sufficiently above (Tg), where the polymer network possesses adequate segmental mobility and stress relaxation is predominantly controlled by the kinetics of dynamic bond exchange. Close to (Tg), however, segmental mobility changes strongly with temperature and becomes coupled with the bond-exchange process. Consequently, the relaxation response is no longer governed solely by the same kinetic behavior observed at higher temperatures, and extrapolation of the high-temperature isoconversional parameters into this region becomes less reliable.

The results at 140–150 °C therefore define an important limitation of the kinetic model. Rather than indicating that stress relaxation ceases near (Tg), the experimental results show that relaxation still occurs, but its time dependence is not adequately reproduced by the Arrhenius-based isoconversional description obtained from the higher-temperature regime. For this reason, predictions of stress-relaxation behavior close to or below the glass transition region should be interpreted with caution, and the TTT map developed subsequently is most physically meaningful within the temperature range in which the kinetic assumptions remain valid.

The DMA results demonstrate two important characteristics of the vitrimer relaxation process. First, at temperatures sufficiently above (Tg), stress relaxation is strongly thermally activated and is satisfactorily described by the Friedman isoconversional approach. Second, the progressive increase in apparent activation energy with conversion reveals that the kinetics evolve continuously as the network relaxes rather than being governed by a single constant activation barrier. At temperatures approaching (Tg), additional restrictions associated with segmental mobility become significant and the isoconversional predictions increasingly deviate from the experimental response. These observations define the temperature range over which the extracted kinetic parameters can be reliably applied and provide the stress-relaxation kinetics subsequently combined with the independently determined thermal-degradation kinetics in the construction of the time–temperature–transformation map.

3.4. Time–Temperature–Transformation (TTT) Map

3.4.1. Construction of the TTT Diagram

Figure 3-6 presents the time–temperature–transformation (TTT) diagram constructed for the studied epoxy vitrimer by combining the stress-relaxation kinetics obtained from DMA with the thermal-degradation kinetics obtained from TGA. Both processes were characterized independently using Friedman's isoconversional method, allowing the time required to reach a prescribed degree of stress relaxation or thermal degradation to be predicted as a function of temperature. By representing both processes on the same time–temperature coordinates, the diagram provides a direct comparison between the kinetics of the desired vitrimeric network rearrangement and those of the competing irreversible degradation process.

The blue curves represent the predicted isoconversional contours of the stress-relaxation process. Each contour corresponds to a specific degree of stress relaxation, ranging from 10% to 90%. For a given temperature, the position of each contour indicates the time required for the material to reach the corresponding relaxation level. As expected for a thermally activated process, the relaxation times decrease strongly with increasing temperature. At relatively low temperatures, several orders of magnitude in time are required to achieve substantial stress relaxation, whereas at temperatures above approximately 200 °C the same relaxation levels are reached within considerably shorter times.

Among the stress-relaxation contours, the 63% relaxation curve is highlighted because it corresponds to the conventional characteristic relaxation time, τ^*. For an ideal single-exponential relaxation process, τ^*corresponds to the time at which the remaining normalized stress has decreased to approximately $1/e$, meaning that approximately 63% of the initial stress has been relaxed. Although the present vitrimer exhibits conversion-dependent relaxation kinetics rather than a single constant relaxation time, the 63% contour remains a useful reference for comparison with conventional vitrimer characterization.

The red curves represent the predicted thermal-degradation contours corresponding to degradation degrees of 0.1%, 1%, and 5%. Each degradation contour defines the combination of temperature and exposure time required to reach that particular degradation level. As in the stress-relaxation process, the degradation kinetics are strongly temperature dependent: increasing temperature substantially reduces the time required to reach a given degree of

degradation. However, the degradation contours are generally located at longer times than the stress-relaxation contours over much of the temperature range investigated.

The relative positions of the blue and red curves are particularly important for defining the practical processing and reprocessing behavior of the vitrimer. At a given temperature, stress relaxation can occur before a significant degree of thermal degradation is accumulated. For example, a processing condition located after a selected stress-relaxation contour but before a chosen degradation contour represents a time–temperature window in which substantial network rearrangement can be achieved while maintaining degradation below the corresponding threshold. The region separating the relaxation and degradation contours therefore provides a kinetic window for vitrimer reprocessing.

The width of this processing window depends strongly on temperature and on the selected criteria for acceptable relaxation and degradation. A less demanding relaxation target, such as 30 or 40%, can be reached considerably earlier than 80 or 90% relaxation, whereas adopting a stricter degradation limit, such as 0.1%, reduces the available processing time compared with a 1 or 5% degradation threshold. Consequently, there is no single universal reprocessing condition; instead, the appropriate time and temperature must be selected according to the degree of network relaxation required and the maximum tolerable level of irreversible degradation.

The horizontal dashed line indicates the glass transition temperature, T_g, of the pristine vitrimer. This temperature provides an important reference for interpreting the stress-relaxation predictions. As shown in the preceding DMA analysis, the Friedman-based stress-relaxation predictions reproduce the experimental behavior satisfactorily at temperatures sufficiently above T_g, but increasing deviations are observed as the temperature approaches the glass-transition region. Close to T_g, segmental mobility becomes increasingly restricted and the relaxation response is no longer governed solely by the same Arrhenius-type kinetic behavior observed at higher temperatures. The stress-relaxation contours near this region should therefore be interpreted with caution, and the most reliable application of the TTT diagram lies at temperatures sufficiently above T_g.

The secondary vertical axis expresses the stress-relaxation times in terms of an equivalent viscosity. This conversion provides an alternative interpretation of the vitrimer response by relating the relaxation timescale to the effective flow resistance of the network. As temperature decreases and relaxation becomes progressively slower, the corresponding

viscosity increases by several orders of magnitude, reflecting the transition from a readily rearranging network at high temperature to an effectively frozen network at lower temperature.

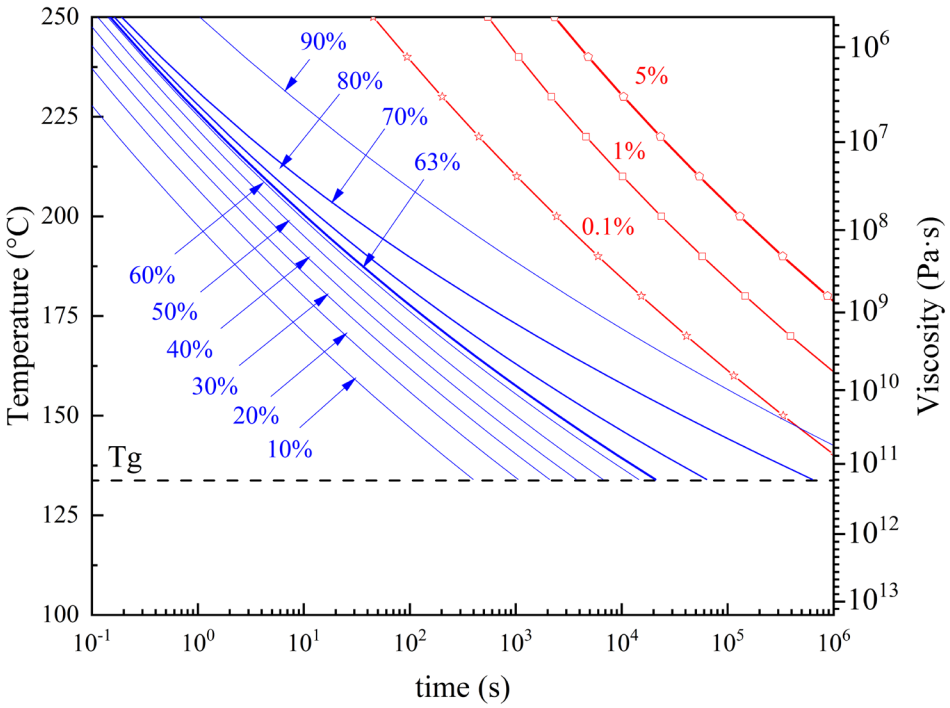


Figure 3-6 Time–temperature–transformation (TTT) diagram showing the predicted stress-relaxation and thermal-degradation kinetics of the epoxy vitrimer

The TTT diagram summarizes the kinetic competition that governs vitrimer processing. Increasing temperature accelerates the dynamic bond-exchange reactions responsible for stress relaxation and therefore favors faster reprocessing, but it simultaneously accelerates irreversible thermal degradation. Reprocessing conditions must consequently be selected within a region where sufficient stress relaxation can occur before an unacceptable degree of degradation is reached. The combined representation of stress-relaxation and degradation kinetics therefore provides a practical framework for identifying suitable time–temperature conditions for the processing and reprocessing of the studied epoxy vitrimer.

3.4.2. Selection of Oven-Treatment Conditions from the TTT Map

The TTT diagram presented in the previous section was used to select the thermal exposure conditions for generating specimens with different degrees of degradation. A treatment temperature of 220 °C was selected as a suitable compromise between accelerating thermal

degradation to experimentally accessible times and avoiding excessively rapid degradation that could severely damage the specimens before subsequent characterization. At this temperature, the degradation contours shown in the TTT diagram indicate that measurable degradation develops progressively with increasing exposure time, allowing several distinct degradation states to be produced within a practical experimental period.

Five experimental conditions were considered: an undegraded reference specimen (0 h) and specimens thermally treated at 220 °C for 30 min, 1 h, 2 h, and 4 h (Figure 3-7). The untreated specimen was retained as the pristine reference and was not subjected to the oven treatment. The remaining specimens were placed in the oven at the same time and exposed to the same constant temperature of 220 °C. Individual specimens were then removed sequentially after their prescribed exposure times: the first after 30 min, the second after 1 h, the third after 2 h, and the final specimen after 4 h.

Using a single treatment temperature for all degraded specimens was a deliberate experimental choice. In this way, the thermal exposure temperature remained constant throughout the specimen series, while treatment time was the only systematically varied parameter. Consequently, differences subsequently observed in the thermal and viscoelastic properties of the specimens can be related more directly to the progressive accumulation of thermal degradation rather than to simultaneous changes in both temperature and exposure time.

The selected exposure times were intended to cover a sufficiently broad range of degradation states, from relatively limited thermal exposure at 30 min to substantially more prolonged exposure after 4 h. This approach also enables the experimentally measured degradation levels to be compared with the degradation kinetics predicted from the Friedman isoconversional analysis. Rather than assuming that a particular exposure time corresponds directly to a fixed degree of degradation, the actual degradation state of each specimen can subsequently be quantified and related to its measured material properties.

It should also be noted that, according to the TTT diagram, stress relaxation at 220 °C occurs on a considerably shorter timescale than the selected oven-treatment durations. Therefore, the dynamic bond-exchange processes responsible for vitrimeric stress relaxation are expected to be highly active during the thermal treatment. However, the primary purpose of these oven exposures was not to investigate stress relaxation itself, but to generate a controlled series of thermally degraded specimens that could subsequently be used to

evaluate the influence of degradation on the glass transition temperature and viscoelastic behavior of the material.

Overall, the treatment conditions of 220 °C for 0, 0.5, 1, 2, and 4 h provide a systematic experimental series in which progressively increasing thermal exposure can be related to the resulting degree of degradation and, subsequently, to changes in the physical and viscoelastic properties of the epoxy vitrimer.

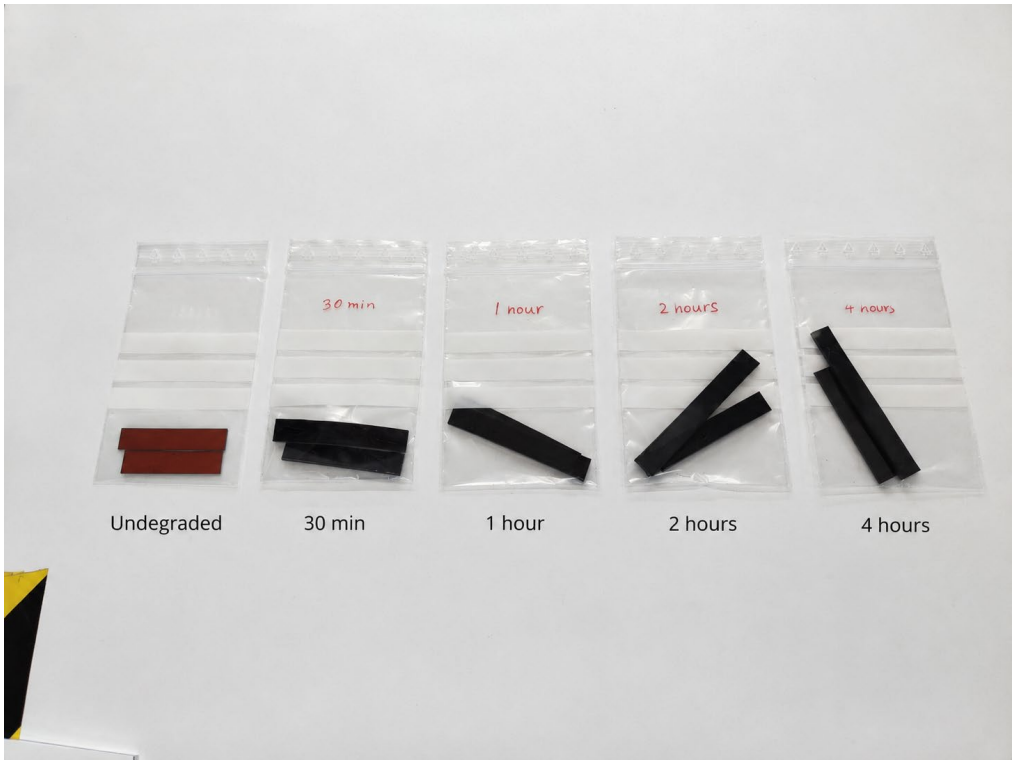


Figure 3-7 Visual appearance of the pristine and thermally treated epoxy vitrimer specimens after exposure at 220 °C for 30 min, 1 h, 2 h, and 4 h. The undegraded specimen is shown on the left

3.5. Evolution of Storage Modulus with Degradation

3.5.1. E' vs. Degradation Time from DMA Double-Cantilever Measurements

Figure 3-8 presents the evolution of the mean storage modulus, E', of the epoxy vitrimer as a function of thermal degradation time at 220 °C. The storage modulus was obtained from DMA measurements performed in the double-cantilever configuration.

The undegraded specimens exhibit the highest mean storage modulus, with a value of approximately 5430 MPa. However, this condition also shows the largest experimental

scatter, with the error bar extending approximately from 3750 to 7100 MPa. The relatively large variability of the pristine specimens should therefore be considered when comparing the absolute magnitude of the modulus reduction with the thermally treated conditions.

Following 30 min of exposure at 220 °C, the mean E'decreases markedly to approximately 3800 MPa. A further decrease is observed after 1 h, for which the mean storage modulus is approximately 3500 MPa, and after 2 h, where the lowest mean value of approximately 3240 MPa is obtained. Overall, the results from 0 to 2 h therefore indicate a progressive reduction in stiffness with increasing thermal exposure time.

Compared with the undegraded reference, the mean storage modulus after 2 h is approximately 40% lower. Although the large scatter associated with the undegraded specimens limits the certainty of the absolute reduction relative to the initial condition, the progressive decrease observed between the 30 min, 1 h, and 2 h conditions indicates that prolonged thermal exposure generally leads to a reduction in the elastic response of the vitrimer.

Interestingly, this decreasing trend is not maintained at the longest exposure time. After 4 h at 220 °C, the mean storage modulus increases to approximately 3950 MPa, representing a partial recovery relative to the 2 h condition. The corresponding error bar is comparatively small, suggesting that this increase is reproducible within the tested specimens rather than being solely a consequence of experimental scatter.

The evolution of $E'$with degradation time is therefore non-monotonic. An initial decrease in storage modulus is observed up to 2 h of thermal exposure, followed by an increase after 4 h. This indicates that the mechanical response of the vitrimer cannot be described simply by a continuous loss of stiffness with increasing treatment time. While the initial decrease is consistent with progressive alteration of the polymer network during thermal degradation, the increase observed at longer exposure suggests that additional structural changes may become relevant at more advanced stages of thermal treatment. These possible mechanisms are discussed in the following section.

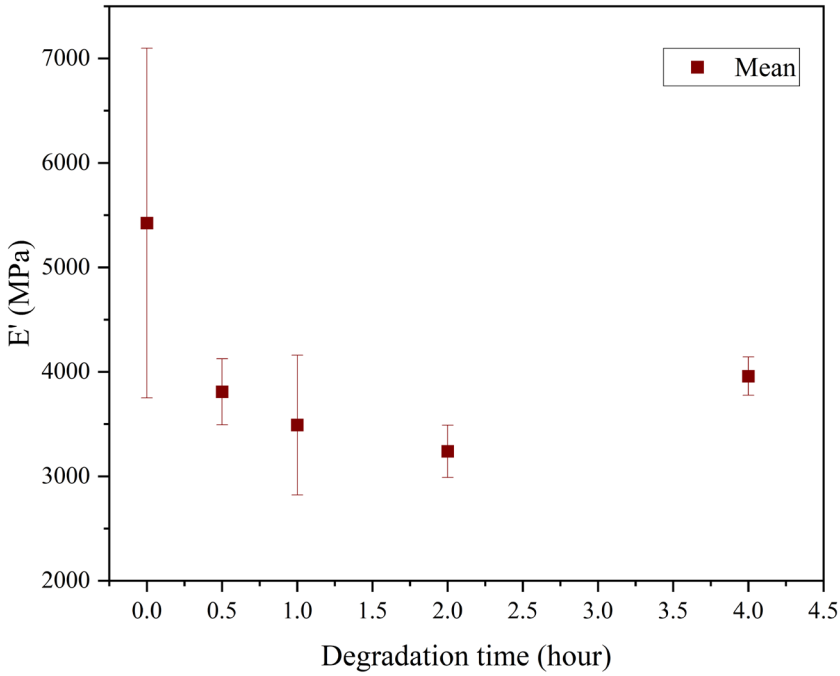


Figure 3-8 Evolution of the storage modulus, (E'), with degradation time for pristine and thermally degraded epoxy vitrimer specimens treated at 220 °C

3.5.2. Discussion: Stiffness Loss Mechanisms

A likely contribution to the stiffness reduction is the progressive loss of effective network connectivity caused by thermally induced bond scission. In a cross-linked epoxy network, the mechanical stiffness depends strongly on the integrity of the three-dimensional molecular structure. Cleavage of covalent bonds within the network generates shorter or less constrained molecular segments and increases their local mobility, thereby reducing the resistance of the material to deformation. In the present vitrimer, this effect is particularly relevant because the network contains dynamic aromatic disulfide bonds, whose thermal stability must be considered at elevated temperatures. Prolonged thermal exposure can therefore involve both the reversible exchange reactions responsible for vitrimeric behavior and irreversible reactions that progressively alter the original network structure. The thesis literature review similarly identifies the susceptibility of disulfide-containing networks to thermally induced changes.

The progressive reduction in E'up to 2 h is also consistent with the thermal-degradation kinetics determined from the TGA and Friedman analyses. Although the conventional TGA curves show the major mass-loss process beginning at substantially higher temperatures during continuous heating, the oven treatment is performed isothermally for periods of up to

several hours. Thermal degradation is a kinetic process; therefore, temperatures below the apparent degradation onset observed during a heating ramp can still produce measurable structural changes when the exposure time is sufficiently long. The TTT analysis accounts specifically for this combined influence of temperature and time.

The behavior after 4 h is more complex. Instead of continuing to decrease, the mean storage modulus increases to approximately 3950 MPa. Consequently, the complete evolution of $E'$is non-monotonic, consisting of an initial stiffness reduction followed by a partial increase at the longest treatment time. This increase should not be interpreted as recovery of the original material, since the 4 h specimen has undergone a substantially longer thermal exposure and its modulus remains below that of the undegraded reference. Rather, it suggests that additional structural changes may become important during prolonged treatment.

One possible explanation is the occurrence of secondary reactions within the thermally aged network. After initial bond scission, reactive degradation products or remaining functional groups may undergo further reactions during prolonged exposure, potentially producing additional crosslinks or more rigid structures. Because the oven treatment is carried out under ambient conditions, oxidative reactions may also contribute to the evolution of the network [53]. Such processes could locally increase rigidity and partially compensate for the stiffness loss produced during the earlier stages of degradation. The pronounced darkening of the thermally treated specimens with increasing exposure time is consistent with substantial chemical modification of the material, although the visual change alone cannot identify the reactions responsible.

Dynamic disulfide exchange may also contribute to the evolution of the network during the thermal treatment. At 220 °C, the TTT diagram indicates that stress relaxation occurs on a much shorter timescale than the oven exposures used here. Thus, extensive bond exchange and topological rearrangement are expected to occur before the specimens are removed from the oven. Because disulfide exchange is associative, this process does not necessarily reduce the number of crosslinks directly; instead, it changes their connectivity and allows the network topology to reorganize. Such rearrangement may interact with simultaneous irreversible degradation and could contribute to the non-monotonic mechanical response. However, DMA alone cannot separate the effects of bond exchange, irreversible chain scission, oxidation, or possible secondary crosslinking.

Experimental variability must also be considered. The undegraded condition exhibits a substantially larger error bar than the thermally treated specimens, and therefore the magnitude of the stiffness decrease relative to the pristine value should be interpreted cautiously. Nevertheless, the relatively narrow error bars at 2 and 4 h, together with the clear increase in the corresponding mean values, suggest that the change between these two conditions is not simply associated with the large variability observed for the pristine specimens.

The results indicate that the mechanical consequences of prolonged thermal exposure cannot be described by a simple monotonic relationship in which increasing degradation time continuously reduces stiffness. During the initial treatment period, the dominant effect appears to be a loss of effective network integrity, producing a progressive decrease in E'. At longer exposure times, additional structural transformations appear to partially counteract this stiffness loss. However, without complementary chemical characterization, such as FTIR, Raman spectroscopy, or analysis of changes in network chemistry, the precise origin of the increase observed after 4 h cannot be established conclusively. The result should therefore be regarded as evidence of a change in the dominant structural response of the material rather than as proof of a specific degradation mechanism.

3.6. Evolution of Glass Transition Temperature with Degradation

3.6.1. Tg vs. Degree of Thermal Degradation

Figure 3-9 presents the evolution of the glass transition temperature, T_g, as a function of the degree of thermal degradation. For this analysis, fully cured vitrimer samples were thermally treated at 220 °C to reach different target degradation levels selected from the degradation-kinetics predictions. The glass transition temperature of each degraded sample was subsequently determined by differential scanning calorimetry (DSC). Expressing T_g directly as a function of the degree of degradation allows the influence of thermal degradation on the polymer network to be evaluated independently of the specific exposure time.

A pronounced decrease in T_g is observed during the initial stages of degradation. At the lowest degradation level, approximately 1%, the highest measured T_g is around 118 °C. As degradation increases, T_g decreases rapidly, with values of approximately 108 °C at around 1–

2% degradation, approximately 103 °C near 2%, and approximately 97 °C at around 3% degradation. By approximately 4% degradation, T_g has decreased to about 89 °C.

The decrease continues more gradually until a minimum of approximately 88 °C is reached at around 6% degradation. Overall, the initial degradation region therefore corresponds to a substantial reduction in T_g, from approximately 118 °C to 88 °C. This represents a decrease of about 30 °C, demonstrating that the glass transition temperature of the vitrimer is highly sensitive to relatively small degrees of thermal degradation.

At higher degradation levels, however, the evolution of T_g becomes non-monotonic. Between approximately 6 and 10% degradation, the glass transition temperature increases again, rising from approximately 88 °C to around 92 °C at 8% degradation and reaching approximately 95 °C near 10% degradation. A subsequent decrease is then observed, with T_g falling to approximately 93 °C at around 10.5% degradation and finally to approximately 88 °C at the highest degradation level investigated, approximately 12.5%.

The overall relationship between T_g and degradation is therefore characterized by two distinct regions. The first, extending approximately from 1 to 6% degradation, is dominated by a strong decrease in T_g. Beyond approximately 6%, the trend becomes more complex, with a partial increase in T_g followed by a second decrease at the highest degradation level. Consequently, the effect of thermal degradation on the glass transition cannot be represented by a simple continuously decreasing relationship across the full degradation range.

The red curve shown in Figure 3-9 is included as a guide to illustrate this overall non-monotonic evolution. It should not be interpreted as a kinetic or constitutive model of the degradation process, but rather as a visual representation of the trend observed experimentally.

Interestingly, this non-monotonic behavior is qualitatively similar to that observed for the storage modulus, E', where the stiffness initially decreased with thermal exposure before partially increasing at the longest treatment condition. The occurrence of similar changes in two independently measured viscoelastic properties suggests that the network undergoes more complex structural evolution at advanced degradation levels than would be expected from simple progressive bond scission alone. The possible mechanisms responsible for this behavior are discussed in the following section.

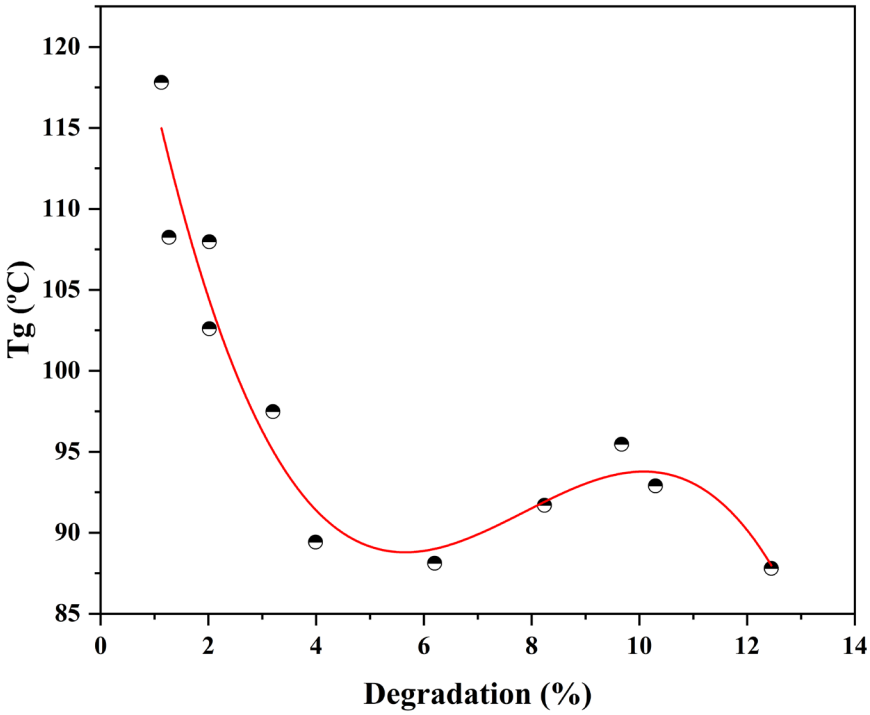


Figure 3-9 Glass transition temperature, (Tg), as a function of the degree of thermal degradation for pristine and thermally degraded epoxy vitrimer specimens

3.6.2. Discussion: Correlating Tg Loss with Network Degradation Kinetics

The evolution of the glass transition temperature with degradation provides a direct indication of how progressive thermal damage modifies the molecular mobility of the epoxy vitrimer network. As shown in Figure 3-9, the most pronounced change occurs during the initial degradation range, where T_g decreases from approximately 118 °C at around 1% degradation to approximately 88–89 °C at 4–6% degradation. A reduction of nearly 30 °C over this relatively limited degradation interval demonstrates that the glass transition temperature is highly sensitive to the early stages of thermal damage.

This initial decrease is consistent with a progressive reduction in the effective connectivity of the cross-linked network. The glass transition of a thermosetting polymer is strongly influenced by the restrictions imposed on segmental molecular motion. In a highly connected network, chain segments are constrained by the surrounding covalent structure and a relatively high temperature is required to achieve the molecular mobility associated with the glass transition. Thermal degradation introduces irreversible changes into this structure, including bond scission and the formation of less constrained molecular segments. As the

effective network connectivity decreases, segmental motion becomes possible at lower temperatures and T_g consequently decreases.

This interpretation is particularly relevant for the present material because its network incorporates aromatic disulfide bonds, which are responsible for the dynamic exchange behavior of the vitrimer but also participate in the thermally activated evolution of the network. The literature reviewed in this dissertation identifies the thermal stability of the S–S bond as an important limitation of disulfide-containing vitrimer systems. Nevertheless, the present TGA and DMA measurements do not independently identify which specific chemical bonds are cleaved at each degradation level. The observed decrease in T_g should therefore be interpreted more generally as evidence of a progressive loss or alteration of effective network constraints rather than as direct proof of cleavage of one particular bond type.

The T_g evolution can also be compared with the conversion-dependent degradation kinetics obtained from Friedman's isoconversional analysis. The apparent activation energy was approximately 200 kJ·mol^{-1} over the early degradation region before progressively decreasing as α approached approximately 0.05–0.07. This variation showed that the degradation process is not governed by a single constant kinetic barrier, but evolves as degradation proceeds. The strong decrease in T_g over approximately the first 4–6% degradation occurs within the same general conversion range in which the Friedman analysis indicates a change in the effective degradation kinetics. This correspondence suggests that the kinetic evolution detected by TGA has a measurable consequence at the macroscopic material level: as degradation accumulates, the molecular network becomes progressively less effective at restricting segmental motion.

At approximately 6% degradation, however, the trend changes. Rather than continuing to decrease, T_g partially recovers, rising from approximately 88 °C to approximately 95 °C near 10% degradation. This behavior cannot be explained by a simple model of continuously increasing chain scission. If thermal exposure only caused a progressive loss of network connectivity, increasing degradation would normally be expected to produce a continued reduction in T_g. The partial increase therefore indicates that additional structural processes become significant at more advanced degradation levels.

Interestingly, this transition occurs close to the region where the Friedman analysis also shows its most pronounced change in apparent activation energy. Around $\alpha \approx 0.07$, E_α reaches a

local minimum before increasing again toward higher conversion. The coincidence between the change in the T_g trend and the non-monotonic evolution of $E_\alpha$suggests that the dominant degradation behavior of the material may be changing in this region. Rather than a single degradation pathway operating throughout the process, several reactions or structural transformations may contribute with different relative importance as degradation progresses. A similar non-monotonic response was observed independently in the storage modulus measurements. E'decreased during the earlier stages of thermal treatment and then increased after the longest exposure condition. The fact that both T_g and E' initially decrease and subsequently exhibit a partial recovery supports the interpretation that the network undergoes a more complex structural evolution at advanced degradation levels rather than simple continuous loss of crosslink density. The existing thesis results likewise show this corresponding non-monotonic behavior in the two measured properties.

One possible explanation is that prolonged thermal exposure promotes secondary reactions among the remaining network fragments or degradation products, producing structures that restrict molecular mobility more strongly than those present immediately after the initial degradation stage. Oxidative reactions may also contribute because the thermal treatments were conducted under ambient oven conditions. Such changes could increase the effective rigidity or connectivity of portions of the degraded network and therefore produce a partial increase in T_g. However, this interpretation remains a hypothesis because the present experimental techniques do not provide direct chemical identification of the structures formed during prolonged thermal exposure. Techniques such as FTIR, Raman spectroscopy, or chemical analysis of the degraded network would be required to establish the underlying chemical mechanism conclusively.

The subsequent decrease in $T_g$to approximately 88 °C at the highest measured degradation level, around 12.5%, further demonstrates that the apparent recovery is temporary and should not be interpreted as restoration of the original polymer network. It is also important to note that this highest degradation level extends beyond the principal $\alpha \leq 0.10$ range examined in the Friedman analysis. Therefore, a direct kinetic interpretation of this final data point using the extracted E_α values should be made cautiously.

From a practical perspective, the most important result is the large reduction in $T_g$produced during the initial stages of degradation. A loss of approximately 30 °C by only 4–6%

degradation implies that relatively modest thermal degradation can substantially reduce the temperature range over which the vitrimer retains its original glassy behavior. This is particularly important for structural applications, since a lower T_g means that increased segmental mobility and the associated reduction in stiffness can begin at significantly lower service temperatures.

Overall, the results establish a direct relationship between the thermal-degradation kinetics and the evolution of the glass transition temperature. The initial degradation stage is accompanied by a strong reduction in T_g, consistent with progressive loss of effective network constraints. At higher degradation levels, the non-monotonic behavior of T_g, together with the corresponding variation in apparent activation energy and storage modulus, indicates that additional structural transformations become important. Consequently, thermal degradation in this vitrimer cannot be described simply as a continuously increasing amount of network damage producing a proportional decrease in T_g; instead, both the degradation kinetics and the resulting material properties evolve as the network structure changes.

3.7. Linking Degradation Kinetics to Physical Property Loss

The results obtained in this work establish a direct connection between the thermal-degradation kinetics of the epoxy vitrimer and the resulting evolution of its thermal and viscoelastic properties. Rather than describing degradation only in terms of exposure temperature and time, the approach adopted here combines kinetic analysis with direct measurements of storage modulus and glass transition temperature. This makes it possible to relate the progressive transformation of the polymer network to measurable changes in material performance.

The multi-heating-rate TGA experiments first demonstrated that thermal degradation is a strongly temperature-dependent and kinetically controlled process. Increasing the heating rate systematically shifted the mass-loss curves toward higher temperatures, while the overall multi-stage shape of the degradation response remained similar. Application of Friedman's isoconversional method showed that this process cannot be described using a single constant activation energy. After the less reliable very-low-conversion region, the apparent activation energy reached approximately 200 kJ·mol^{-1} and remained relatively stable over the early degradation range before decreasing toward higher conversion, including a distinct minimum

around $\alpha \approx 0.07$, followed by a partial increase. The degradation kinetics therefore evolve progressively as the transformation proceeds.

A similar conversion-dependent behavior was identified for the stress-relaxation process using DMA. At temperatures sufficiently above the glass transition region, the experimentally measured relaxation response was satisfactorily represented by the Friedman isoconversional approach, confirming that the dynamic network rearrangement is strongly thermally activated. At temperatures closer to T_g, however, increasing deviations were observed between the experimental response and the isoconversional prediction, indicating that restrictions in segmental mobility become increasingly important and that simple extrapolation of the higher-temperature Arrhenius behavior becomes less reliable.

The independently determined stress-relaxation and degradation kinetics were subsequently combined in the TTT diagram. This representation shows directly the competition between the desired dynamic bond-exchange process and irreversible thermal degradation. At a given temperature, substantial stress relaxation can occur before a selected degradation threshold is reached, defining a time–temperature region in which the vitrimer network can undergo rearrangement while degradation remains limited. This balance is particularly important for aromatic disulfide-containing vitrimer networks because the same dynamic chemistry that enables stress relaxation and reprocessing must operate under elevated-temperature conditions where irreversible thermal changes can also occur. The studied network contains dynamic aromatic disulfide bonds capable of thermally activated exchange.

Based on this kinetic framework, a treatment temperature of 220 °C was selected to generate specimens with progressively increasing thermal exposure. An undegraded reference condition was compared with specimens treated for 30 min, 1 h, 2 h, and 4 h. Maintaining a constant temperature while varying only the exposure time provided a systematic series of degradation conditions from which the consequences of prolonged thermal treatment could be evaluated.

The storage-modulus measurements revealed a clear physical consequence of the initial degradation process. The mean E'decreased from approximately 5430 MPa for the undegraded material to approximately 3800 MPa after 30 min, 3500 MPa after 1 h, and 3240 MPa after 2 h. This represents an overall reduction of approximately 40% relative to the mean value of the pristine material. Although the relatively large variability of the undegraded condition requires some caution when interpreting the exact magnitude of this reduction, the

progressive decrease between the thermally treated conditions indicates a clear loss of stiffness during the initial stages of exposure.

An even stronger relationship was observed between the degree of degradation and the glass transition temperature. T_g decreased from approximately 118 °C at the lowest degradation level to approximately 88–89 °C at around 4–6% degradation, corresponding to a reduction of almost 30 °C. This large decrease over a comparatively small degradation interval demonstrates that the thermal transition of the material is highly sensitive to early degradation. In practical terms, even a relatively limited degree of degradation can therefore substantially reduce the temperature at which significant segmental mobility develops.

The simultaneous decrease in $E'$and T_g during the initial degradation region provides a coherent indication of progressive alteration of the cross-linked network. Both properties are strongly influenced by molecular constraints: storage modulus reflects the resistance of the network to deformation, whereas T_g reflects the temperature at which sufficient segmental mobility becomes possible. A reduction in effective network connectivity therefore provides a consistent physical explanation for the simultaneous decrease of both quantities. Previous studies summarized in the literature review similarly show that excessive thermal exposure of epoxy systems can reduce glass transition temperature and mechanical properties.

Importantly, however, neither property continues to decrease monotonically at the most advanced degradation conditions. After reaching its minimum at 2 h, the storage modulus increases to approximately 3950 MPa after 4 h. Similarly, T_g increases from approximately 88 °C near 6% degradation to approximately 95 °C at around 10% degradation before decreasing again to approximately 88 °C at the highest degradation level investigated. Thus, both independently measured properties display an initial deterioration followed by a partial recovery at more advanced degradation.

This non-monotonic behavior corresponds qualitatively with the evolution of the apparent degradation activation energy. The pronounced change in $E_\alpha$around intermediate conversion, particularly the minimum observed near $\alpha \approx 0.07$, occurs in approximately the same degradation region in which the evolution of the physical properties begins to depart from the initial monotonic trend. This correspondence suggests that the change detected kinetically by the Friedman analysis has a physical manifestation in the material response. As degradation progresses, the relative importance of the reactions and structural transformations occurring within the network appears to change.

Nevertheless, the partial increases in E' and T_g at higher degradation should not be interpreted as recovery of the original material. Thermal degradation is irreversible, and the specimens at these conditions have experienced substantially greater thermal exposure than the reference material. The increase instead indicates that the structure of the degraded network has evolved into a state with different mechanical and molecular-mobility characteristics. Secondary reactions, oxidative processes, or thermally induced rearrangement of the remaining network may contribute to this behavior, but the precise chemical origin cannot be established from TGA and DMA measurements alone.

The combined results therefore suggest two broad regimes of material response. During the initial degradation regime, extending approximately to 4–6% degradation, increasing degradation is associated with a pronounced and comparatively consistent reduction in both stiffness and glass transition temperature. This is the region of greatest practical importance because relatively modest degradation already produces substantial deterioration of the original material properties. At more advanced degradation levels, a second, more complex regime develops in which the physical properties no longer follow a simple monotonic relationship with mass loss, indicating that additional structural transformations become significant.

This distinction is important when using the TTT diagram to define processing and reprocessing conditions. A degradation threshold should not be selected solely on the basis of whether the specimen remains macroscopically intact. The present results demonstrate that appreciable reductions in T_g and stiffness can already occur at comparatively low levels of degradation. Consequently, the safe processing window should ideally be selected so that sufficient stress relaxation is achieved while remaining within the early part of the degradation regime, before significant deterioration of the original network properties occurs.

Overall, the combined kinetic and property measurements demonstrate that the degree of thermal degradation provides a meaningful parameter for assessing the consequences of thermal exposure in the studied epoxy vitrimer. The Friedman analysis describes how rapidly degradation develops under different time–temperature conditions, while DMA reveals the corresponding change in stiffness, while DSC provides the evolution of the glass transition temperature. By combining these results with the stress-relaxation kinetics in the TTT framework, the present work extends the concept of a processing window beyond simply predicting whether degradation will occur: it provides a basis for assessing how much

degradation can be tolerated before the physical performance of the vitrimer is significantly altered. This directly addresses the central objective of establishing a quantitative relationship between thermal degradation and the resulting viscoelastic and thermal behavior of the material.

4. CONCLUSION

4.1. Summary of Findings

This dissertation investigated the effect of thermal degradation on the glass transition temperature and viscoelastic behavior of an aromatic disulfide-based epoxy vitrimer. Thermal degradation and stress-relaxation kinetics were independently characterized using TGA and DMA, respectively, and analyzed using Friedman's isoconversional method. The resulting kinetic descriptions were combined in a time–temperature–transformation (TTT) diagram to identify the competition between the dynamic bond-exchange process required for reprocessing and irreversible thermal degradation.

The results demonstrate that both degradation and stress relaxation are conversion-dependent processes and cannot be adequately represented by a single constant activation energy. The stress-relaxation kinetics were satisfactorily described by the isoconversional approach at temperatures sufficiently above T_g. However, as the temperature approached the glass-transition region, increasing deviations between the experimental and predicted relaxation behavior were observed. Near T_g, segmental mobility becomes strongly temperature dependent and increasingly coupled with the dynamic bond-exchange process, so the simple Arrhenius-type description underlying the present isoconversional treatment is no longer sufficient. Understanding and modelling this transition region remains an important problem, and further investigation of this behavior is currently part of ongoing state-of-the-art research.

Controlled thermal treatments at 220 °C demonstrated that relatively small degrees of degradation can already lead to substantial changes in material performance. During the initial degradation regime, approximately up to 4–6% degradation, both storage modulus and T_g decreased markedly. At higher degradation levels, both properties showed a non-monotonic response, suggesting that additional structural transformations become important as degradation progresses. Therefore, the physical consequences of thermal exposure cannot be described by a simple proportional relationship between mass loss and property

deterioration. Most importantly, the results show that a material may remain macroscopically intact while its thermal and viscoelastic performance has already been significantly altered.

The present work also complements the cure-kinetics characterization developed in previous work for this vitrimer system. Considered together, the cure kinetics, stress-relaxation kinetics, and degradation kinetics provide the basis for a more complete description of the material throughout its processing and reprocessing cycle. The next step is therefore to integrate these kinetic processes with the experimentally established evolution of T_g and mechanical properties, so that processing maps can define not only whether curing or reprocessing is kinetically possible, but also whether the resulting material retains an acceptable level of performance. This extends the TTT concept from a purely kinetic tool toward a property-based processing and reprocessing framework.

4.2. Future Work

Further work should focus on improving the description of stress relaxation in the vicinity of T_g, where the present isoconversional model becomes less reliable, and on identifying the chemical mechanisms responsible for the non-monotonic behavior observed at advanced degradation. Complementary techniques such as FTIR, Raman spectroscopy, or other chemical and structural characterization would help distinguish between irreversible bond scission, oxidation, secondary reactions, and network rearrangement. In addition, the present investigation was carried out on the neat vitrimer resin, and an important next step is to extend the same kinetic and property-based methodology to fiber-reinforced vitrimer composites. The presence of fibers can modify heat transfer, constrain matrix deformation, influence stress relaxation, and alter the development and consequences of thermal degradation. Evaluating the combined fiber–resin system would therefore be necessary to determine whether the processing and reprocessing windows identified for the neat resin remain valid at the composite scale and to assess how degradation affects composite-level properties such as stiffness, interfacial integrity, damage tolerance, and reprocessability. Additional degradation conditions and larger experimental datasets would also strengthen the quantitative relationship between degradation degree and material performance.

This work demonstrates that defining a safe processing or reprocessing window for an epoxy vitrimer requires consideration not only of how rapidly the network can cure or relax and how

rapidly it degrades, but also of how that degradation affects the properties required for service. Combining cure, stress-relaxation, degradation, and property-evolution kinetics provides a more complete basis for the design of processing, reprocessing, and lifetime-management strategies for aromatic disulfide-based epoxy vitrimers. Extending this framework from the neat resin to fiber-reinforced composite systems represents an important next step toward its application in structural composite materials.

References

[1] D. Sanchez-Rodriguez *et al.*, "Time-temperature-transformation diagrams from isoconversional kinetic analyses applied to the processing and reprocessing of vitrimers," *Thermochimica Acta,* vol. 736, p. 179744, 2024.

[2] O. Becker, Y.-B. Cheng, R. J. Varley, and G. P. Simon, "Layered silicate nanocomposites based on various high-functionality epoxy resins: the influence of cure temperature on morphology, mechanical properties, and free volume," *Macromolecules,* vol. 36, no. 5, pp. 1616-1625, 2003.

[3] H. Sukanto, W. W. Raharjo, D. Ariawan, J. Triyono, and M. Kaavesina, "Epoxy resins thermosetting for mechanical engineering," *Open Engineering,* vol. 11, no. 1, pp. 797-814, 2021.

[4] J. Yang *et al.*, "High-toughness, environment-friendly solid epoxy resins: Preparation, mechanical performance, curing behavior, and thermal properties," *Journal of Applied Polymer Science,* vol. 137, no. 17, p. 48596, 2020.

[5] W. Post, A. Susa, R. Blaauw, K. Molenveld, and R. J. Knoop, "A review on the potential and limitations of recyclable thermosets for structural applications," *Polymer reviews,* vol. 60, no. 2, pp. 359-388, 2020.

[6] T. Liu, B. Zhao, and J. Zhang, "Recent development of repairable, malleable and recyclable thermosetting polymers through dynamic transesterification," *Polymer,* vol. 194, p. 122392, 2020.

[7] A. La Rosa *et al.*, "Life cycle assessment of a novel hybrid glass-hemp/thermoset composite," *Journal of cleaner production,* vol. 44, pp. 69-76, 2013.

[8] C. J. Kloxin, T. F. Scott, B. J. Adzima, and C. N. Bowman, "Covalent adaptable networks (CANs): a unique paradigm in crosslinked polymers," *Macromolecules,* vol. 43, no. 6, p. 2643, 2010.

[9] C. N. Bowman and C. J. Kloxin, "Covalent adaptable networks: reversible bond structures incorporated in polymer networks," *Angewandte Chemie International Edition,* vol. 51, no. 18, pp. 4272-4274, 2012.

[10] C. J. Kloxin and C. N. Bowman, "Covalent adaptable networks: smart, reconfigurable and responsive network systems," *Chemical Society Reviews,* vol. 42, no. 17, pp. 7161-7173, 2013.

[11] N. Nishiie, R. Kawatani, S. Tezuka, M. Mizuma, M. Hayashi, and Y. Kohsaka, "Vitrimer-like elastomers with rapid stress-relaxation by high-speed carboxy exchange through conjugate substitution reaction," *Nature Communications,* vol. 15, no. 1, p. 8657, 2024.

[12] S. Jin, D. X. Oh, and J. Park, "Dynamic Disulfide Chemistry for Functional Polymers: Self-Healing, Vitrimer Behavior, and Biochemical/Electronic Applications," *ChemSusChem,* vol. 19, no. 1, p. e202501023, 2026.

[13] I. C. Cabrera, "Epoxy vitrimer materials based on disulfide exchange chemistry: experimental study and modeling of the stress relaxation-application to composites reinforced by nanofibrillated cellulose," Université de Toulon, 2021.

[14] Y. Zuo, Z. Gou, C. Zhang, and S. Feng, "Polysiloxane-Based Autonomic Self-Healing Elastomers Obtained through Dynamic Boronic Ester Bonds Prepared by Thiol–Ene “Click” Chemistry," *Macromolecular rapid communications,* vol. 37, no. 13, pp. 1052-1059, 2016.

[15] D. Montarnal, M. Capelot, F. Tournilhac, and L. Leibler, "Silica-like malleable materials from permanent organic networks," *Science,* vol. 334, no. 6058, pp. 965-968, 2011.

[16] W. Denissen, G. Rivero, R. Nicolaÿ, L. Leibler, J. M. Winne, and F. E. Du Prez, "Vinylogous urethane vitrimers," *Advanced Functional Materials,* vol. 25, no. 16, pp. 2451-2457, 2015.

[17] A. Ruiz de Luzuriaga *et al.*, "Epoxy resin with exchangeable disulfide crosslinks to obtain reprocessable, repairable and recyclable fiber-reinforced thermoset composites," *Materials Horizons,* vol. 3, no. 3, pp. 241-247, 2016.

[18] M. Capelot, M. M. Unterlass, F. Tournilhac, and L. Leibler, "Catalytic control of the vitrimer glass transition," *ACS Macro Letters,* vol. 1, no. 7, pp. 789-792, 2012.

[19] J. Zheng *et al.*, "Vitrimers: Current research trends and their emerging applications," *Materials Today,* vol. 51, pp. 586-625, 2021.

[20] M. Guerre, C. Taplan, J. M. Winne, and F. E. Du Prez, "Vitrimers: directing chemical reactivity to control material properties," *Chemical science,* vol. 11, no. 19, pp. 4855-4870, 2020.

[21] N. J. Van Zee and R. Nicolaÿ, "Vitrimers: Permanently crosslinked polymers with dynamic network topology," *Progress in Polymer Science,* vol. 104, p. 101233, 2020.

[22] Y. Yang, Y. Xu, Y. Ji, and Y. Wei, "Functional epoxy vitrimers and composites," *Progress in Materials Science,* vol. 120, p. 100710, 2021.

[23] F. Meng, M. O. Saed, and E. M. Terentjev, "Rheology of vitrimers," *Nature communications,* vol. 13, no. 1, p. 5753, 2022.

[24] W. Alabiso and S. Schlögl, "The impact of vitrimers on the industry of the future: chemistry, properties and sustainable forward-looking applications," *Polymers,* vol. 12, no. 8, p. 1660, 2020.

[25] B. Krishnakumar, R. P. Sanka, W. H. Binder, V. Parthasarthy, S. Rana, and N. Karak, "Vitrimers: Associative dynamic covalent adaptive networks in thermoset polymers," *Chemical Engineering Journal,* vol. 385, p. 123820, 2020.

[26] W. Post, A. Cohades, V. Michaud, S. Van Der Zwaag, and S. Garcia, "Healing of a glass fibre reinforced composite with a disulphide containing organic-inorganic epoxy matrix," *Composites Science and Technology,* vol. 152, pp. 85-93, 2017.

[27] J. M. Matxain, J. M. Asua, and F. Ruipérez, "Design of new disulfide-based organic compounds for the improvement of self-healing materials," *Physical Chemistry Chemical Physics,* vol. 18, no. 3, pp. 1758-1770, 2016.

[28] S. Nevejans, N. Ballard, J. I. Miranda, B. Reck, and J. M. Asua, "The underlying mechanisms for self-healing of poly (disulfide) s," *Physical Chemistry Chemical Physics,* vol. 18, no. 39, pp. 27577-27583, 2016.

[29] A. Rekondo, R. Martin, A. Ruiz de Luzuriaga, G. Cabanero, H. J. Grande, and I. Odriozola, "Catalyst-free room-temperature self-healing elastomers based on aromatic disulfide metathesis," *Materials Horizons,* vol. 1, no. 2, pp. 237-240, 2014.

[30] Z. Q. Lei, H. P. Xiang, Y. J. Yuan, M. Z. Rong, and M. Q. Zhang, "Room-temperature self-healable and remoldable cross-linked polymer based on the dynamic exchange of disulfide bonds," *Chemistry of Materials,* vol. 26, no. 6, pp. 2038-2046, 2014.

[31] I. Azcune, A. Huegun, A. R. de Luzuriaga, E. Saiz, and A. Rekondo, "The effect of matrix on shape properties of aromatic disulfide based epoxy vitrimers," *European Polymer Journal,* vol. 148, p. 110362, 2021.

[32] I. Azcune and I. Odriozola, "Aromatic disulfide crosslinks in polymer systems: Self-healing, reprocessability, recyclability and more," *European Polymer Journal,* vol. 84, pp. 147-160, 2016.

[33] V. Schenk, K. Labastie, M. Destarac, P. Olivier, and M. Guerre, "Vitrimer composites: current status and future challenges," *Materials Advances,* vol. 3, no. 22, pp. 8012-8029, 2022.

[34] Y. Li, Y. Zhang, O. Rios, J. K. Keum, and M. R. Kessler, "Liquid crystalline epoxy networks with exchangeable disulfide bonds," *Soft Matter,* vol. 13, no. 29, pp. 5021-5027, 2017.

[35] L. Zhang, L. Chen, and S. J. Rowan, "Trapping dynamic disulfide bonds in the hard segments of thermoplastic polyurethane elastomers," *Macromolecular Chemistry and Physics,* vol. 218, no. 1, p. 1600320, 2017.

[36] X. Jian, Y. Hu, W. Zhou, and L. Xiao, "Self-healing polyurethane based on disulfide bond and hydrogen bond," *Polymers for Advanced Technologies,* vol. 29, no. 1, pp. 463-469, 2018.

[37] T. Liu *et al.*, "A self-healable high glass transition temperature bioepoxy material based on vitrimer chemistry," *Macromolecules,* vol. 51, no. 15, pp. 5577-5585, 2018.

[38] D. Sánchez-Rodríguez *et al.*, "Processability and reprocessability maps for vitrimers considering thermal degradation and thermal gradients," *Polymer Degradation and Stability,* vol. 217, p. 110543, 2023.

[39] X. Yang, L. Guo, X. Xu, S. Shang, and H. Liu, "A fully bio-based epoxy vitrimer: Self-healing, triple-shape memory and reprocessing triggered by dynamic covalent bond exchange," *Materials & Design,* vol. 186, p. 108248, 2020.

[40] Y. Yang, Z. Pei, X. Zhang, L. Tao, Y. Wei, and Y. Ji, "Carbon nanotube–vitrimer composite for facile and efficient photo-welding of epoxy," *Chemical Science,* vol. 5, no. 9, pp. 3486-3492, 2014.

[41] Z. Yang, Q. Wang, and T. Wang, "Dual-triggered and thermally reconfigurable shape memory graphene-vitrimer composites," *ACS applied materials & interfaces,* vol. 8, no. 33, pp. 21691-21699, 2016.

[42] N. S. Dosoudil, "Investigation of vitrimer epoxy resins for carbon fiber reinforced polymers and fiber metal laminates," Dissertation, Augsburg, Universität Augsburg, 2022, 2022.

[43] A. Takahashi, T. Ohishi, R. Goseki, and H. Otsuka, "Degradable epoxy resins prepared from diepoxide monomer with dynamic covalent disulfide linkage," *Polymer,* vol. 82, pp. 319-326, 2016.

[44] L. Sorrentino, L. Esposito, and C. Bellini, "A new methodology to evaluate the influence of curing overheating on the mechanical properties of thick FRP laminates," *Composites Part B: Engineering,* vol. 109, pp. 187-196, 2017.

[45] A. Doblies, B. Boll, and B. Fiedler, "Prediction of thermal exposure and mechanical behavior of epoxy resin using artificial neural networks and Fourier transform infrared spectroscopy," *Polymers,* vol. 11, no. 2, p. 363, 2019.

[46] B. J. Anderson, "Thermal stability and lifetime estimates of a high temperature epoxy by Tg reduction," *Polymer degradation and stability,* vol. 98, no. 11, pp. 2375-2382, 2013.

[47] R. Carbas, L. F. da Silva, E. Marques, and A. Lopes, "Effect of post-cure on the glass transition temperature and mechanical properties of epoxy adhesives," *Journal of Adhesion Science and Technology,* vol. 27, no. 23, pp. 2542-2557, 2013.

[48] R. Carbas, E. Marques, L. F. da Silva, and A. Lopes, "Effect of cure temperature on the glass transition temperature and mechanical properties of epoxy adhesives," *The Journal of Adhesion,* vol. 90, no. 1, pp. 104-119, 2014.

[49] G. Berčič, "The universality of Friedman's isoconversional analysis results in a model-less prediction of thermodegradation profiles," *Thermochimica Acta,* vol. 650, pp. 1-7, 2017.

[50] W. H. Press, *Numerical recipes 3rd edition: The art of scientific computing*. Cambridge university press, 2007.

[51] J. Farjas and P. Roura, "Isoconversional analysis of solid-state transformations: A critical review. Part III. Isothermal and non isothermal predictions," *Journal of thermal analysis and calorimetry,* vol. 109, no. 1, pp. 183-191, 2012.

[52] S. Rasi, P. Roura-Grabulosa, and J. Farjas, "Application of thermal analysis and kinetic predictions to YBCO films prepared by chemical solution deposition methods: S. Rasi et al," *Journal of Thermal Analysis and Calorimetry,* vol. 142, no. 5, pp. 2077-2086, 2020.

[53] D. Apostolidis, P. Jayaraman, C. A. Dransfeld, B. Kumru, and N. Lorenz, "Linking Process-Induced Degradation to Mechanical Property Deterioration in Flax Fiber–Reinforced Bio-Polymer Matrix Composites," *Polymer Composites,* vol. 47, no. 10, pp. 9377-9391, 2026.